Vanadium(II) Salts in Pyridine and Acetonitrile Solvents

Phalguni Ghosh,[†,‡] Henry Taube,*[,‡] Tai Hasegawa,[‡] and Reiko Kuroda[§]

Departments of Chemistry, Stanford University, Stanford, California 94305, and College of Arts and Sciences, University of Tokyo, Komaba, Tokyo 153, Japan

Received March 31, 1995[⊗]

Earlier work on the interaction of V(II) salts with pyridine and acetonitrile as solvents has been extended. The structure of the compound $VPy_4(O_3SCF_3)_2$, **1**, an intermediate in many of the preparations, has been determined by X-ray diffraction. Analogous solids with I^-, Br^-, Cl^-, SCN^-, N_3^-, PhS^-, EtS^-, and BH_4^- as counterions have been prepared. Attempts to prepare solids with PhO^-, HO^-, MeO^-, Ph^-, CN^-, AlH_4^-, and H^- failed, but the tetrapyridine complexes were prepared by titrating a solution of **1** in pyridine with the lithium salt of each anion (in the case of H^-, the anion was Et_3BH^-) to an end point observed at the 1:2 ratio. Comparisons in a number of cases of the absorption spectra and of the cyclovoltammetric behavior of the tetrapyridine salts in pyridine and in CH_2Cl_2 show the species in the two solvents to be the same and to correspond to the composition of the solids. Intercomparisons of the absorption spectra in pyridine suggest that the complexes with the aforementioned anions all have similar structures: four pyridine molecules situated equatorially—on the basis of crystal structure determinations, in a propeller arrangement—and the anions occupying axial positions. The initial absorption spectrum of a solution of $VPy_4(PF_6)_2$ in pyridine changes to that shown by a solution of $VPy_6(PF_6)_2$ or of $VPy_6(BPh_4)_2$, and we conclude that with these weakly nucleophilic anions VPy_6^{2+} is the dominant form of V(II) in pyridine solution. In every case, the prominent feature of the absorption spectrum is a band envelope consisting of a maximum that ranges from 586 to 400 nm accompanied by a shoulder which usually lies on the low-energy side of the dominant peak and which in these cases we assign to ν_{CT} and ν_1'', respectively. The latter is the higher energy component of the two transitions ν_1' and ν_1'', which arise from ν_1 (octahedral) when the symmetry is reduced to axial. Energy correlations suggest that ν_{CT} always lies at higher energy than ν_1'', so that when the shoulder lies on the high-energy side of the dominant peak, $\epsilon(\nu_1'')$ exceeds $\epsilon(\nu_{CT})$. In a number of cases ν_1' is observed. It is of much lower intensity than ν_1'', and the wavelengths of the transitions lie in the range of 600 nm and higher and vary with the nature of ligands as observed in other cases of axial symmetry. The absorption characteristics of VPy_6^{2+} resemble those of the tetrapyridine complexes, suggesting that the propeller-like arrangement is retained in this species, two pyridines replacing the anions in the axial positions; i.e., the axial and equatorial pyridines are inequivalent.

Introduction

The work reported here is an extension of earlier work on the chemistry of vanadium in nonaqueous, more particularly nonprotic, solvents.[1,2] The long-range goal of this program is to develop selective reactions of O_2 with organic substrates. The hope is that, by relying on catalysis by vanadium species, such reactions can proceed under mild conditions. In line with this goal, we were drawn to studying the basic chemistry of vanadium in selected solvents. Considerations which led to the choice of the lowest common oxidation state, namely V(II), for early study are the following: Vanadium(II) is a strong reducing agent, and this property combined with the fact that each of three πd orbitals is occupied suggests that back-bonding effects would be significant. These have barely been touched upon for a πd^3 system—in fact little has been done along these lines for any paramagnetic center—and it was hoped the comparisons of the effects observed with V(II) in pyridine and acetonitrile as solvents, the molecules of which have π acid character, with those of the more thoroughly investigated πd^6 systems (Ru(II)) would prove to be instructive.

The major thrust of the work was to characterize the dominant forms of a variety of V(II) salts in the two solvents. Though some V(II) salts similar to those we have prepared have been described, there has not been much emphasis on the issue of the nature of the species in solution. Having this in hand is an essential requirement in understanding the reaction chemistry. Because the species are likely to be substitution labile in solution, there is no guarantee that the constitution in solution will be the same as that in the solid. The six papers by Larkworthy et al.[3] deal with spectra and magnetic properties in the solid state. Measurements of the electronic absorption spectra of VCl_2 in THF, CH_3OH, Py, and CH_3CN have been reported,[4] but no effort was made to establish the compositions of the species in solution. This applies also to some measurements of solution spectra reported for imidazole complexes of V(II).[5] In a series of papers by Cotton and co-workers,[6] the emphasis is on the structure of the solid phases. The structures

† Present address: The Scripps Research Institute, La Jolla, CA 92037.
‡ Stanford University.
§ University of Tokyo.
⊗ Abstract published in *Advance ACS Abstracts,* September 15, 1995.
(1) Dobson, J. C.; Sano, M.; Taube, H. *Inorg. Chem.* **1991**, *30*, 456.
(2) Dobson, J. C.; Taube, H. *Inorg. Chem.* **1989**, *28*, 1310.
(3) (a) Khamar, M. M.; Larkworthy, L. F.; Patel, K. C.; Phillips, D. J.; Beech, G. *Aust. J. Chem.* **1974**, *27*, 41. (b) Larkworthy, L. F.; Patel, K. C.; Phillips, D. J. *J. Chem. Soc. A* **1970**, 1095. (c) Larkworthy, L. F.; Tucker, B. J. *Inorg. Chim. Acta* **1978**, *33*, 167. (d) Larkworthy, L. F.; O'Donoghue, M. W. *Inorg. Chim. Acta* **1983**, *71*, 81. (e) Holt, D. G. L.; Larkworthy, L. F.; Povey, D. C.; Smith, G. W.; Leigh, G. J. *J. Chem. Soc., Dalton Trans.* **1990**, 3229. (f) Holt, D. G. L.; Larkworthy, L. F.; Povey, D. C.; Smith, G. W.; Leigh, G. J. *Inorg. Chim. Acta* **1990**, *169*, 201.
(4) Seifert, H. J.; Auel, T. *J. Inorg. Nucl. Chem.* **1968**, *30*, 2081.
(5) Ciampolini, M.; Mani, F. *Inorg. Chim. Acta* **1977**, *24*, 91.
(6) (a) Cotton, F. A.; Duraj, S. A.; Manjer, L. E.; Roth, W. J. *J. Am. Chem. Soc.* **1985**, *107*, 385. (b) Cotton, F. A.; Duraj, S. A.; Roth, W. J. *Inorg. Chem.* **1985**, *24*, 913. (c) Cotton, F. A.; Duraj, S. A.; Roth, W. J.; Schmulbach, C. D. *Inorg. Chem.* **1985**, *24*, 525. (d) Cotton, F. A.; Poli, R. *Inorg. Chim. Acta* **1988**, *141*, 91.

0020-1669/95/1334-5761$09.00/0

of some phosphine complexes of V(II), as determined by X-ray diffraction, have been reported.[7] The studies reported by Maverick and co-workers[8] are an exception to the emphasis in most of the other work on the nature of the solid state species.

Glossary: DME, 1,2-dimethoxyethane; DMPE, (dimethylphosphino)ethane; TBAHP, tetrabutylammonium hexafluorophosphate; TBAOTf, tetrabutylammonium trifluoromethanesulfonate; THF, tetrahydrofuran.

Experimental Section

Materials. Vanadium trichloride, trifluoromethanesulfonic acid, ethyl isonicotinate, 4-ethylpyridine, DMPE, and all inorganic lithium salts, except LiSPh and LiSEt, were purchased from Aldrich Chemical Co. Lithium thiophenolate was prepared by the reaction of a stoichiometric amount of LiOMe with thiophenol in methanol solution. The precipitated solid was washed with cold methanol and dried. The lithium salt of ethyl mercaptan was obtained by refluxing the THF solution of ethanethiol with lithium metal for 48 h under an inert atmosphere. Vanadium tribromide was purchased from Johnson and Matthey. Tetra-*n*-butylammonium hexafluorophosphate (TBAHP) and tetra-*n*-butylammonium trifluoromethanesulfonate (TBAOTf), electrochemical grade, were purchased from Fluka and Aldrich Chemical Co. Diethyl ether and toluene, Aldrich Sure Seal bottle, <0.005% water, was used as received. Dichloromethane, reagent grade, was purified by the following procedure: It was stirred overnight with concentrated sulfuric acid, after which it was separated from the acid layer, washed with saturated aqueous $NaHCO_3$, followed by aqueous saturated KOH/KCl and distilled water, and then dried over anhydrous $K_2CO_3/MgSO_4$, the final stage being distillation from CaH_2. Acetonitrile, reagent grade, was treated as described in the literature.[9] Pyridine, reagent grade, was treated by distillation from solid KOH, followed by distillation from CaH_2. Tetrahydrofuran was dried by distillation from $LiBH_4$, and methanol, by distillation from $Mg(OCH_3)_2$. All solvents were deoxygenated by purging with argon, and reactions were carried out under an argon atmosphere in a Vacuum Atmosphere glovebox or by using standard Schlenk techniques.

UV−vis spectra were recorded in a quartz cell or cuvette on either a Beckman Model 5270 spectrophotometer or a Hewlett-Packard Model 8452 A diode array spectrophotometer. Infrared spectra were recorded on an IBM 98 FTIR spectrometer. NMR spectra were measured in CD_2Cl_2 or C_5D_5N on a Nicolet (300 MHz) NMR spectrophotometer. Chemical shifts are reported as δ values downfield from an internal standard of Me_4Si. Cyclic voltammetric experiments were performed in a Vacuum Atmospheres glovebox using a PAR Model 173 potentiostat with a PAR Model 175 universal programmer as a sweep generator. Measurements were made in a cell fitted with a Pt or glassy carbon working electrode, a platinum auxiliary electrode, and a reference consisting of an Au button electrode immersed in an acetonitrile or DME solution containing 1 M TBAHP, the reference compartment being separated from the main cell by a Vycor frit. Unless otherwise indicated, the supporting electrolyte was TBAHP (0.10 M) and the concentration of V(II) was 1.0×10^{-3} M. No correction was made for junction potential effects. The potential window for pyridine containing the electrolyte was −1.8 to +1.2 V. The reference for each of the solvents used was calibrated with the ferrocene/ferrocenium couple ($E = 0.55$ V vs NHE). All elemental analyses were performed by Galbraith Laboratories Inc., Knoxville, TN, and/or Micro Analytic, Tucson, AZ, and the analytical results are supplied as Supporting Information. Unless otherwise stated, operations were carried out at room temperature.

Synthesis of Compounds. The complexes $V(O_3SCF_3)_3$ and $V(THF)_4(O_3SCF_3)_2$ were prepared by following the literature procedures.[10,11] In the case of the latter compound, analysis of the crystalline material showed that zinc ion formed during the reduction cocrystallizes with V(II) compounds to the extent of ca. 5%.

$VPy_4(O_3SCF_3)_2$ (1). The reaction solution was made up by dissolving $V(THF)_4(O_3SCF_3)_2$ (light blue crystals, 0.16 mmol) in 50 mL of hot pyridine with stirring. After 2 h, the dark solution was filtered through a fine glass frit, and the volume of the liquid was reduced to 15 mL. Dark brown crystals appeared, which were collected by filtration and dried under vacuum. Yield: 85 mg (80%).

VPy_4Cl_2. Method 1. The procedure followed is described in the literature.[12]

Method 2. Solid lithium chloride, 13.4 mg (0.31 mmol), was added to a 10 mL pyridine solution of 100 mg (0.15 mmol) of $VPy_4(O_3SCF_3)_2$, and the reaction mixture was stirred overnight (stirring is necessary in many cases because of the limited solubility of the lithium reagent). The resulting purple solution was filtered, and recrystallization was induced by vapor diffusion into the filtrate, diethyl ether being used as a precipitant. Yield: 60 mg (87%).

VPy_4X_2. The derivatives with $X = Br^-$, I^-, and SCN^- were prepared by following method 2. The average yield was 60−80% for the crystalline materials. When CN^-, HO^-, MeO^-, PhO^-, Ph^-, or CH_3^- was used as a coligand, isolation as a crystalline material was not successful (see Results).

$VPy_4(SPh)_2$. Lithium thiophenolate, 36.7 mg (0.32 mmol), was added to a solution of 100 mg (0.15 mmol) of $V(Py)_4(O_3SCF_3)_2$ in 3 mL of pyridine, and the resulting mixture was kept stirring overnight. Then 15 mL of diethyl ether was added, the mixture was filtered, and the filtrate was stored at −10 °C overnight. Dark red crystals deposited on the wall of the container. These were collected by filtration and washed with diethyl ether. Yield: 55 mg (65%).

$VPy_4(N_3)_2$. A solution of 100 mg (0.15 mmol) of $V(Py)_4(O_3SCF_3)_2$ in 5 mL of pyridine was prepared, and 20.5 mg (0.32 mmol) of NaN_3 was added to it. The reaction mixture was allowed to stir for 12 h, and the resulting deep red solution was evaporated to dryness. The red mass was dissolved in 5 mL of cold CH_2Cl_2, the solution was filtered, and the solvent was removed completely under vacuum, the solid then being redissolved in 3 mL of pyridine. The product was precipitated with diethyl ether and dried. Yield: 42 mg (50%).

$VPy_4(BH_4)_2 \cdot CH_2Cl_2$. A solution of $LiBH_4$ in THF (0.17 ml, 2.0 M) was added to a solution of 100 mg (0.15 mmol) of $VPy_4(O_3SCF_3)_2$ in 6 mL of CH_2Cl_2, and the reaction mixture was stirred for 3 h and stored at −10 °C in a refrigerator overnight. The white precipitate which resulted during the reaction was filtered off and discarded. Two drops of pyridine were added to the orange-red filtrate, followed by 5 mL of diethyl ether. Dark brown crystals were deposited on the wall of the container after 3 days at −10 °C. These were collected by filtration and dried. Yield: 32 mg (55%).

$V(4\text{-}EtPy)_4(O_3SCF_3)_2$. The synthesis followed that described for $VPy_4(O_3SCF_3)_2$. The final yield was 75 mg (80%).

$V(4\text{-}EtPy)_4Cl_2$. Dark crystals were obtained from a 4-EtPy/Et_2O (1:4; v/v) solvent mixture by method 1 as described for the preparation of $V(Py)_4Cl_2$. Yield: 80%.

$V(4\text{-}EtPy)_4(BH_4)_2$. The procedure was the same as that for $VPy_4(BH_4)_2$.

$V(4\text{-}EtPy)_4I_2$. This compound was synthesized by following method 2 as used for VPy_4Cl_2 except that diethyl ether was used as a reaction medium instead of pyridine. On addition of more LiI, a brick red solid promptly appeared in almost quantitative yield. Yield: 90 mg (95%).

V(ethyl isonicotinate)$_4$(O$_3$SCF$_3$)$_2$. This dark orange solid was isolated by following the procedure described for $VPy_4(O_3SCF_3)_2$, with ethyl isonicotinate instead of pyridine being used as reagent. Yield: 75 mg (85%).

$VPy_6(PF_6)_2$. A solution of $AgPF_6$ in acetonitrile (2.5 mmol in 5 mL) was added slowly, at room temperature, to a suspension of 1.15

(7) (a) Girolami, G. S.; Wilkinson, G.; Galas, A. M. R.; Thornton-Pett, M.; Hursthouse, M. B. *J. Chem. Soc., Dalton Trans.* **1985**, 1339. (b) Girolami, G. S.; Jensen, J. A. *J. Am. Chem. Soc.* **1988**, *110*, 4450. (c) Anderson, S. J.; Wilkinson, G.; Hussain, B.; Hursthouse, M. B. *Polyhedron* **1988**, *7*, 2614.

(8) (a) Shah, S. S.; Maverick, A. W. *Inorg. Chem.* **1987**, *26*, 1559. (b) Maverick, A. W.; Shah, S. S.; Kirmaier, C.; Holten, D. *Inorg. Chem.* **1987**, *26*, 774. (c) Shah, S. S.; Maverick, A. W. *Inorg. Chem.* **1986**, *25*, 1867. (d) Shah, S. S.; Maverick, A. W. *J. Chem. Soc., Dalton Trans.* **1987**, 2881.

(9) Perrin, D. D.; Armareago, W. L. F. In *Purification of Laboratory Chemicals*, 3rd ed.; Pergamon Press: New York, 1988; p 68.

(10) Singh, S.; Gill, A. M. S.; Verma, R. D. *J. Fluorine Chem.* **1985**, *27*, 2429.

(11) Scott, M. J.; Wolf, C.; Wilisch, A.; Armstrong, W. H. *J. Am. Chem. Soc.* **1990**, *112*, 2430.

(12) Edema, J. J. H.; Stauthamer, W.; Bolhuis, F.; Gambarotta, S.; Smeets, W. J. J.; Spek, A. L. *Inorg. Chem.* **1990**, *29*, 1302.

mmol of $V(CH_3CN)_4Cl_2$ in 10 mL of acetonitrile. A white precipitate appeared immediately, and the solution became green. The mixture was stirred for 3 h to ensure completion of the reaction and was then filtered. The solution volume was reduced to 2 mL under vacuum, and the resulting bluish green precipitate was collected by filtration and dried. It was suspended in 10 mL of pyridine, and the mixture was stirred for 48 h and then filtered. The solvent was removed under vacuum, and the residue was dissolved again with another 10 mL portion of pyridine and the solution was stirred for another 24 h. On the addition of 20 mL of diethyl ether to the dark brown solution, a light yellow-brown precipitate formed. This was collected and dried. Yield: 280 mg (70%).

$VPy_5(PF_6)_2$. The title compound resulted when $VPy_6(PF_6)_2$ was subjected to high vacuum-drying for 24 h at room temperature. Yield: 100%.

$VPy_4(PF_6)_2$. Crystals (100 mg) of $V(CH_3CN)_6(PF_6)_2$ were added to 20 mL of pyridine, and the mixture was stirred for approximately 3 h. A light greenish yellow precipitate appeared after the addition of 50 mL of diethyl ether with vigorous stirring, which was collected by filtration and dried. Yield: 85 mg (61%).

$VPy_6(BPh_4)_2$. This compound was prepared by the reaction of $V(CH_3CN)_6(BPh_4)_2$ in pyridine (0.10 mmol in 10 mL). Addition of diethyl ether (50 mL) to the mixture after it was stirred for 72 h at room temperature produced a brown oily mass at the bottom of the container. The supernatant liquid was separated from the oil and discarded. After vigorous stirring of the brown oil with 50 mL of diethyl ether, a yellow-brown solid appeared. It was collected and dried under vacuo. Yield: 70%.

$VPy_4(BPh_4)_2 \cdot 2Py$. This compound was prepared by following the procedure described for $VPy_6(BPh_4)_2$, except here the precipitation with diethyl ether was induced after reaction mixture was stirred for only 30 min. The light yellow precipitate was collected and dried. Yield: 60%.

$V(CH_3CN)_6(O_3SCF_3)_2 \cdot 0.5CH_3CN$. The reaction mixture consisted of $V(THF)_4(O_3SCF_3)_2$ (500 mg, 0.78 mmol) dissolved in 10 mL of acetonitrile. It was stirred for 2 h and then evaporated to dryness. The crude material was redissolved in 10 mL of acetonitrile, and the solution was filtered. Crystallization was induced by vapor diffusion into the filtrate with diethyl ether as a precipitant. Dark green crystals were formed along with cube-shaped $Zn(MeCN)_4(O_3SCF_3)_2$ crystals. These were separated mechanically, and the dark green crystals were recrystallized twice from a $MeCN/E_2O$ 1:1 by volume mixture. Yield: 35 mg (40%).

$V(CH_3CN)_6(BPh_4)_2$. The reaction mixture composed of $V(CH_3CN)_4Cl_2$ (0.98 mmol) and Ag_2CO_3(1.3 mmol) in 20 mL of acetonitrile was stirred for 18 h at room temperature and then filtered. A solution of $NaBPh_4$ in CH_3CN, 2.5 mmol in 10 mL, was added to the filtrate with stirring, and the resulting solution was kept at −10 °C overnight. Shining bluish green scaly crystals deposited, which were collected and dried. Yield: 225 mg (25%).

$V(CH_3CN)_6(PF_6)_2$. This compound (crystalline, dark blue) was isolated by following the procedure described for $V(CH_3CN)_6(BPh_4)_2$, but with $AgPF_6$ instead of Ag_2CO_3 being used to remove the Cl^- ion and diethyl ether being added to induce crystallization. Yield: 75%.

$V(CH_3CN)_4Cl_2$. A solution of 100 mg (0.16 mmol) of $V(CH_3CN)_6(O_3SCF_3)_2 \cdot 0.5CH_3CN$ in 15 mL of CH_3CN was prepared, and LiCl (14.3 mg, 0.34 mmol) was added. The mixture was stirred at 40 °C until the dark green color changed to light violet (at least 16 h). It was then filtered, and 15 mL of diethyl ether was added, whereupon a light gray solid appeared, which was precipitated by the addition of diethyl ether. The solid was removed by filtration and dried under vacuum. Yield: 35 mg (75%). The isolated compound is sparingly soluble in acetonitrile.

$V(CH_3CN)_4Br_2$. The synthesis followed the procedure described for the chloride analogue. Yield: 40 mg (65%).

$V(DMPE)_2(O_3SCF_3)_2$. A suspension of 200 mg (0.31 mmol) of $V(THF)_4(O_3SCF_3)_2$ in 15 mL of toluene was stirred for 2 h at 50 °C. A solution of DMPE (0.65 mmol in 1.1 mmol) was added slowly by microsyringe, whereupon a blue color developed. The reaction mixture was heated at 50 °C and was stirred vigorously for 18 h. The resulting pink slurry was dried completely in vacuo and extracted with 50 mL of CH_2Cl_2. Large cube-shaped pink crystals were obtained by the vapor diffusion with diethyl ether as precipitating solvent. Yield: 40 mg (80%).

Table 1. Crystallographic Data for *trans*-$VPy_4(O_3SCF_3)_2$

formula $VC_{22}H_{20}N_4F_6S_2O_6$	space group *Pn* (No. 7)
fw 665.47	$T = 21$ °C
$a = 10.449(1)$ Å	$\mu = 5.61$ cm^{-1}
$b = 9.3088(9)$ Å	$R = 0.055$
$c = 14.620(1)$ Å	$R_w = 0.060$
$\beta = 96.38(1)°$	$Z = 2$
$V = 1413.3(2)$ Å^3	$\rho_{calcd} = 1.564$ g cm^{-3}
cryst syst monoclinic	$\lambda = 0.710\,69$ Å

$V(DMPE)_2Cl_2$. This complex was prepared by following the literature procedure.[7a] Yield: 65%.

$V(DMPE)_2Br_2$. The complex was prepared by following either of the procedures outlined for $V(DMPE)_2Cl_2$ or the route adopted for the $V(DMPE)_2I_2$ preparation (see below). The yield was 60% based on the first procedure.

$V(DMPE)_2I_2$. A solution of lithium iodide (36.8 mg, 0.27 mmol) dissolved in 5 mL of diethyl ether was added to a solution of 85 mg of $V(DMPE)_2(O_3SCF_3)_2$ in 5 mL of CH_2Cl_2, resulting in an immediate change of the deep blue color to light purple. The mixture was kept stirring overnight to complete the reaction. Removal of the solvent under vacuum left an orange-pink solid. This was extracted with 3 mL of CH_2Cl_2, and on the addition of 10 mL of diethyl ether, bright shining orange crystals were deposited on the wall of the container on keeping the solution overnight at −10 °C. The solid was collected by filtration and dried. Yield: 28 mg (35%).

$V(DMPE)_2(Me)_2$. Dark yellow crystals were obtained by following the literature procedure.[7a] Yields: 40%.

$V(DMPE)_2(BH_4)_2$. Red-orange crystals were isolated by following the procedure described by Girolami et al.[7b] Yield: 72%.

Determination of the Crystal Structure of $VPy_4(O_3SCF_3)_2$ (1). Single X-ray-quality crystals were obtained from pyridine and ether as described above. A reddish columnar crystal having the approximate dimensions of 0.3 × 0.6 × 0.45 mm was mounted on a glass fiber. All measurements were made on a Rigaku AFC5S diffractometer with graphite-monochromated Mo Kα radiation and a 12 kW rotating anode generator.

Cell constants and an orientation matrix for data collection, obtained from a least-squares refinement using the setting angles of 25 carefully centered reflections in the range $35.09 < 2\Theta < 38.28°$, corresponded to a monoclinic cell. The dimensions along with other crystallographic data are collected in Table 1. On the basis of the systematic absences, packing considerations, a statistical analysis of intensity distribution, and the successful solution and refinement of the structure, the space group was determined to be *Pn* (No. 7).

The data were collected at a temperature of 21 ± 1 °C using the $\omega-2\Theta$ scan technique to a maximum 2Θ value of 60.0°. ω scans of several intense reflections, made prior to the collection, had an average width at half-height of 0.15° with a takeoff angle of 60.0°. Scans of $(1.52 + 0.30 \tan \Theta)°$ were made at a speed of 8.0°/min (in ω). The weak reflections ($I < 10.0\sigma(I)$) were rescanned (maximum of two rescans), and the counts were accumulated to ensure good counting statistics. Stationary-background counts were recorded on each side of the reflection. The ratio of peak counting time to background counting time was 2:1. The diameter of the incident beam collimator was 0.5 mm, and the crystal to detector distance was 40 cm.

Of the 4714 reflections which were collected, 4350 were unique ($R_{int} = 0.135$); equivalent reflections were merged. The intensities of three representative reflections which were measured after every 150 reflections declined by −11.00%. A linear correction factor was applied to the data to account for this phenomenon. The linear absorption coefficient for Mo Kα is 5.6 cm^{-1}. An empirical absorption correction, using the program DIFABS,[13] was applied, which resulted in transmission factors ranging from 0.77 to 1.20. The data were corrected for Lorentz and polarization effects. The structure was solved by direct methods.[14] The non-hydrogen atoms were refined isotropically. The final cycle of full-matrix least-squares refinement[15] was based on the

(13) DIFABS: Walker, Stuart. *Acta Crystallogr.* **1983**, *A39*, 158−166.

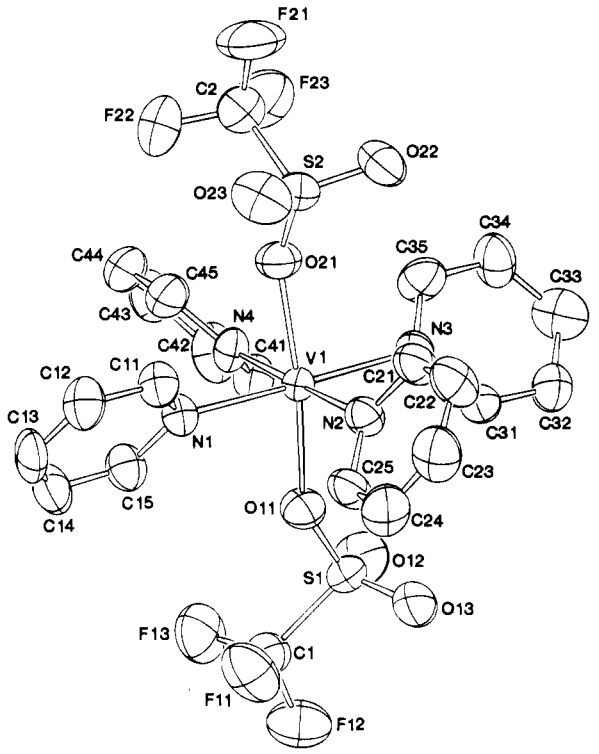

Figure 1. ORTEP diagram of the non-hydrogen atoms of $VPy_4(O_3SCF_3)_2$ (**1**) with 50% probablity thermal ellipsoids.

2553 observed reflections ($I > 3.00\sigma(I)$) and 368 variable parameters and converged with unweighted and weighted agreement factors of $R = \sum||F_o| - |F_c||/\sum|F_o| = 0.055$ and $R_w = [\sum w(|F_o| - |F_c|)^2/\sum wF_o^2]^{1/2} = 0.060$. The standard deviation of an observation of unit weight[16] was 1.94. The weighting scheme was based on counting statistics and included a factor ($p = 0.03$) to downweight the intense reflections. Plots of $\sum w(|F_o| - |F_c|)^2$ versus $|F_o|$, reflection order in data collection, (sin Q)/2, and various classes of indices showed no unusual trends. The maximum and minimum peaks on the final difference Fourier map corresponded to 0.83 and -0.37 e/Å^{-3}, respectively. Neutral-atom scattering factors were taken from Cromer and Waber.[17] Anomalous dispersion effects were included in F_c;[18] the values for $\Delta f'$ and $\Delta f''$ were those of Cromer.[19] All calculations were performed using the TEXSAN[20] crystallographic software package of the Molecular Structure Corp.

Results

Structural Description of *trans*-$VPy_4(O_3SCF_3)_2$. Figure 1 shows the molecular structure of **1**. The complex crystallizes in the monoclinic space group *Pn* with two molecules per unit cell. The crystal data are summarized in Table 1. Selected bond lengths and angles are given in Table 2, and the final positional parameters are given in Table 3. The compound shows the *trans* arrangements of the triflate ligand about the vanadium atoms with the pyridine nitrogen atoms nearly in a plane containing the V(II) ion (±0.015 Å). The axial triflate ligands are slightly distorted from the ideal octahedral arrangement, as is evidenced by the O- -V- -O angle, which is 173.5° rather than 180° (Table 3). The four N- -V- -O angles are unique and range from 85.3 to 94.2°. The dihedral angles between the VN_4 plane and the planes of the pyridine rings are given in Table 4. Complex **1** adopts a "propeller" conformation.[21] The low (C_1) symmetry is enforced by the two unsymmetrical triflate ligands and also by the tilt of the pyridine molecules with respect to the reference VN_4 plane. The dihedral angles between the diagonal pyridine rings (viz. N2−N4 and N1−N3) are 103.11 and 76.35°, respectively. The average V--N distance is 2.187 Å, and the average V- -O distance is 2.128 Å. Table 5 lists intramolecular and intermolecular bond distances within 3 Å between the hydrogen atoms of the pyridine ligands and the electronegative oxygen and fluorine atoms of the triflate ligands. In the Table Va, four O- -H intramolecular distances are less than 2.72 Å, which is the simple sum of their van der Waals radii. Similarly, the closest intermolecular approach distances are F11···H35 = 2.55 Å, F13···H33 = 2.58 Å, O13···H34 = 2.47 Å, and O22···H24 = 2.45 Å (Table Vb). We conclude both intramolecular and intermolecular C−H···X (X = F, O) interactions exist in **1**.

Table 2. Selected Bond Distances and Angles

	Intramolecular Distances (Å)		
V1−O11	2.127(6)	V1−N2	2.199(7)
V1−O21	2.129(6)	V1−N3	2.170(7)
V1−N1	2.194(7)	V1−N4	2.185(7)
	Intermolecular Distances (Å)		
F11−F23	3.11(1)	O12−C12	3.23(1)
F11−C35	3.24(1)	O12−C13	3.27(1)
F11−C34	3.49(1)	O12−C22	3.58(1)
F12−C23	3.41(1)	O13−C43	3.36(1)
F12−O22	3.44(1)	O13−C34	3.41(1)
F12−C24	3.52(1)	O13−C44	3.44(1)
F13−O23	3.019(9)	O22−C24	3.37(1)
F13−C33	3.31(1)	O22−C13	3.41(1)
F13−F21	3.35(1)	O23−C33	3.35(1)
F22−C23	3.23(1)	O23−C32	3.38(1)
F23−C25	3.42(1)		
	Angles (deg)		
O11−V1−O21	173.5(2)	O21−V1−N4	85.3(3)
O11−V1−N1	86.7(2)	N1−V1−N2	89.8(3)
O11−V1−N2	90.0(3)	N1−V1−N3	179.1(3)
O11−V1−N3	94.2(2)	N1−V1−N4	89.9(3)
O11−V1−N4	90.7(3)	N2−V1−N3	90.0(2)
O21−V1−N1	88.2(3)	N2−V1−N4	179.2(3)
O21−V1−N2	93.9(3)	N3−V1−N4	90.3(2)
O21−V1−N3	91.0(3)		

Characterization in Solution. General Information. When solids of well-defined composition were avaible, solutions in pyridine or dichloromethane were prepared from them. In some of the interesting cases, we were limited to preparing the desired compounds by solution procedures. It is impossible to deal with the variety of new species which were so prepared and studied by a simple description which covers them all, and important details will be provided when the individual cases are considered. However, the most widely applied strategy is worth

(14) Structure and solution Methods: (a) Gilmore, C. J. Mithril—an integrated direct methods computer program. *J. Appl. Crystallogr.* **1984**, *17*, 42−46. (b) Beurskens, P. T. DIRDIF: Direct Methods for Difference Structures—an autometic procedure for phase extension and refinement of difference structure factors. Technical Report 1984/1; Crystallography Laboratory: Toernooiveld, 6525 Ed, Nijmegen, The Netherlands, 1984.

(15) Least-Squares: Function minimized $\sum w(|F_o| - |F_c|)^2$, where $w = 4R_o^2/\sigma^2(F_o^2)$, $\sigma^2(F_o^2) = [S^2(C - R^2B) + (pF_o^2)^2]/(Lp)^2$, S = scan rate, C = total integrated peak count, R = ratio of scan time to background counting time, B = total background count, Lp = Lorentz−polarization factor, and $p = p$ factor.

(16) Standard deviation of an observation of unit weight: $[\sum w(|F_o| - |F_c|)^2/(No - Nv)]^{1/2}$, where No = number of observations and Nv = number of variables.

(17) Cromer, D. T.; Waber, J. T. *International Tables for X-ray Crystallography*; The Kynoch Press: Birmingham, England, 1974; Vol. IV, Table 2.2A.

(18) Ibers, J. A.; Hamilton, W. C. *Acta Crystallogr.* **1964**, *17*, 781.

(19) Cromer, D. T.; Waber, J. T. *International Tables for X-ray Crystallography*; The Kynoch Press: Birmingham, England, 1974; Vol. IV, Table 2.3.1A.

(20) TEXAN: *TEXAN Structure Analysis Package*; Molecular Structure Corp.: Woodlands, TX, 1985.

(21) Lipkowski, J. *Inclusion Compounds*; Academic Press: London, 1984; Vol. I, p 59.

Table 3. Positional Parameters and B_{eq} Values for $VPy_4(O_3SCF_3)_2$

atom	x	y	z	B_{eq},[a] Å^2
V1	0.6165	0.9963(1)	0.7132	2.33(3)
S1	0.8414(2)	0.7530(2)	0.6523(2)	3.79(8)
S2	0.4396(2)	1.2483(2)	0.8206(2)	3.79(8)
F11	0.7077(7)	0.5198(6)	0.6196(4)	6.8(3)
F12	0.8880(7)	0.5216(8)	0.5613(5)	8.3(4)
F13	0.7261(7)	0.6458(7)	0.5000(4)	6.8(3)
F21	0.3156(8)	1.4902(7)	0.8049(5)	8.4(4)
F22	0.2848(7)	1.3557(8)	0.6865(5)	8.4(4)
F23	0.4587(7)	1.4718(7)	0.7146(5)	7.6(4)
O11	0.7202(6)	0.8226(7)	0.6622(4)	4.3(3)
O12	0.9237(7)	0.8349(9)	0.6000(5)	6.3(4)
O13	0.8991(8)	0.6888(8)	0.7345(5)	6.5(4)
O21	0.4976(6)	1.1673(6)	0.7507(4)	4.2(3)
O22	0.5313(8)	1.3152(8)	0.8874(5)	6.1(3)
O23	0.3310(7)	1.1774(9)	0.8521(5)	6.0(4)
N1	0.4408(7)	0.8809(8)	0.6598(5)	3.5(3)
N2	0.6159(7)	0.8845(8)	0.8456(5)	3.5(3)
N3	0.7885(7)	1.1125(7)	0.7671(4)	3.3(3)
N4	0.6147(6)	1.1091(8)	0.5820(5)	3.4(3)
C1	0.784(1)	0.604(1)	0.5786(6)	4.6(4)
C2	0.373(1)	1.400(1)	0.7540(8)	5.4(5)
C11	0.3377(7)	0.879(1)	0.7043(6)	3.8(3)
C12	0.2263(8)	0.808(1)	0.6705(6)	4.6(4)
C13	0.2224(9)	0.736(1)	0.5893(7)	4.9(4)
C14	0.327(1)	0.735(1)	0.5437(6)	5.0(4)
C15	0.4350(8)	0.809(1)	0.5791(6)	4.1(4)
C21	0.617(1)	0.9552(9)	0.9249(6)	4.3(4)
C22	0.608(1)	0.887(1)	1.0085(6)	5.0(5)
C23	0.594(1)	0.743(1)	1.0084(8)	5.7(5)
C24	0.594(1)	0.666(1)	0.9284(8)	5.7(5)
C25	0.604(1)	0.7404(9)	0.8476(6)	4.2(4)
C31	0.8962(8)	1.0441(9)	0.8059(6)	4.0(4)
C32	1.0105(8)	1.114(1)	0.8325(7)	4.9(4)
C33	1.017(7)	1.260(1)	0.8228(8)	5.5(5)
C34	0.909(1)	1.331(1)	0.7843(7)	5.2(5)
C35	0.7944(9)	1.255(1)	0.7563(7)	4.7(4)
C41	0.7214(8)	1.120(1)	0.5359(6)	3.9(4)
C42	0.723(1)	1.197(1)	0.4557(6)	5.1(5)
C43	0.614(1)	1.271(1)	0.4207(5)	4.8(4)
C44	0.505(1)	1.260(1)	0.4635(6)	4.9(4)
C45	0.5096(9)	1.181(1)	0.5439(6)	4.5(4)

[a] $B_{eq} = 8\pi^2/3\sum_i\sum_j U_{ij}$, where the general temperature factor expression is $\exp[-2\pi^2(U_{11}h^2a^{*2} + U_{22}k^2b^{*2} + U_{33}l^2c^{*2} + 2U_{12}hka^*b^* + 2U_{13}hla^*c^* + 2U_{23}klb^*c)]$.

Table 4. Dihedral Angles between Least-Squares Planes

1st plane[a]	2nd plane[b]	angle, deg	1st plane[a]	2nd plane[b]	angle, deg
ref	1	52.7	3	1	103.1
ref	2	52.3	3	2	74.6
ref	3	50.6	4	1	109.6
ref	4	51.3	4	2	76.4
2	1	64.6	4	3	120.2

[a] Planes constitute V, N1, N2, N3, and N4 (reference). [b] Plane numbered by N atom number.

outlining at this point. With exceptions to be mentioned, it was to introduce the anionic ligand, usually as the lithium salt dissolved in pyridine, in measured aliquots into a solution of $VPy_4(O_3SCF_3)_2$ in pyridine, noting the appearance of an end point. In most instances this titration procedure succeeded, as it will when the affinities are high and as seems to be true in most instances. The exceptions occur with the weakly nucleophilic anions BPh_4^- and PF_6^-. In some of the cases, as for example with HO^-, CH_3O^-, PhO^-, Ph^-, and CH_3^-, the end point at 2:1 is indicated by the appearance of an intractable solid; in others, the end point is indicated by a "break" in the absorptivity as a function of the ratio of ligand to V(II).

Because of its good solvent characteristics yet low nucleophilicity, CH_2Cl_2 seemed to hold promise as a preparative medium. However, except for solid $VPy_4(BH_4)_2$, which we were unable to prepare in pyridine, presumably because of attack by the base on coordinated BH_4^- [22,23] (vide infra), CH_2Cl_2 was not useful for the preparation of solids which were not accessible in pyridine. With the anions MeO^-, PhO^-, and HO^-, this failure may simply be due to their propensity to function as bridging groups, which leads to ill-defined insoluble condensed products. In the case of Ph^-, the failure is due to a rapid reaction of the nucleophile with the solvent, so that VPy_4Cl_2 rather than the desired product is formed. Surprisingly the tetrapyridine V(II) complexes of N_3^-, EtS^-, and PhS^-, though they can be obtained as solids from pyridine, are found to decompose in CH_2Cl_2.

By following procedures similar to those described, we were unable to prepare VPy_4F_2 as a solid, nor did we find evidence for replacement of $CF_3SO_3^-$ from $VPy_4(O_3SCF_3)_2$ by F^- (introduced as the $[^tBu_4N]F$ salt in pyridine as solvent) at 1.0×10^{-2} M concentration.

Spectrophotometric and Electrochemical Properties in Pyridine Applied to Determining the Species Present in Solution. A summary of spectrophotometric and electrochemical measurements appears in Table 6. They are introduced in parallel because, in some of the most interesting cases, we need to resort to both types of measurements to reach convincing conclusions about the nature of the species.

The first two columns in Table 6 need some explanation. Where solids of defined composition have been obtained and the measurements were made on solutions prepared from them, their compositions appear in the first column. Where no entry in the first column appears, it is to be understood that compositions in solution were arrived at by titration. In the second column, we list the compositions we have inferred for solution species. Where no entry in this column appears opposite the formulas for the solids, it is to be assumed that the composition of the complex in solution is the same as it is in the solid. In some cases, measurements were made on solutions prepared by dissolving the solids in CH_2Cl_2. The entries in Table 6 pertaining to such data are enclosed in brackets.

In applying absorption spectroscopy to establish the nature of the various solutes, we used three different strategies. One was to test whether the solutes obey Beer's law. Where this was applied, the concentration range covered was $(1.0-2.0) \times 10^{-3}$ to $(1.0-1.2) \times 10^{-2}$ M. Adherence to Beer's law proves only that the composition of the V(II) species is invariant on dilution over a particular range in concentration and not necessarily that its composition is the same as in the solid, and it is of limited use on this account. In a number of key instances, the absorption spectra for the species in pyridine were compared to those in CH_2Cl_2. Dichloromethane is a much weaker nucleophile than is pyridine, and the likelihood of its replacing X^- from VPy_4X_2 is very small. A close correspondence of the absorption spectra for VPy_4X_2 in the two solvents is a strong indication that the composition of the solute in both media conforms to that in solid. Because the intense absorption bands have charge transfer character, some differences in λ_{max} and in ϵ arising from changes in solvent must be allowed for. Another approach, already mentioned as being applied when appropriate solids were inaccessible, was to titrate a solution of the triflate salt (this anion is chosen because it is a weak nucleophile and because its salts tend to be quite soluble even in nonprotic

(22) Cotton, F. A.; Wilkinson, G. *Advanced Inorganic Chemistry*, 5th ed.; Wiley: New York, 1988; p 190.
(23) (a) Luetkens, M. L., Jr.; Huffmann, J. C.; Sattelberger, A. P. *J. Am. Chem. Soc.* **1985**, *107*, 3361. (b) Barron, A. R.; Salt, J. E.; Wilkinson, G.; Motevalli, M.; Hursthouse, M. B. *Polyhedron* **1986**, *5*, 1833.

Table 5

(a) Intramolecular Distances and Angles with Hydrogens for $VPy_4(OTf)_2$

A···B—C	A···B, Å	∠ABC, deg	A···B—C	A···B, Å	∠ABC, deg
O11···H15—C15	2.64	109	O21···H21—C21	2.91	109
O11···H25—C25	2.68	113	O21···H35—C35	2.71	112
O11···H31—C31	2.93	107	O21···H45—C45	2.49	119
O11···H41—C41	2.84	107	O23···H21—C21	2.63	152
O12···H41—C41	2.49	160	O23···H11—C11	2.68	148
O13···H31—C31	2.65	144	F13···H15—C15	2.88	144
O21···H11—C11	2.78	107	F22···H45—C45	2.92	144
		van der Waals Radii (Å)			
O···H	2.72		F···H	2.67	

(b) Intermolecular Bond Distances Involving the Non-Hydrogen Atoms for $VPy_4(OTf)_2$

bond	dist, Å	ADC[a]	bond	dist, Å	ADC[a]
F11—F23	3.11(1)	54501	O12—C12	3.23(1)	65501
F11—C35	3.24(1)	54501	O12—C13	3.27(1)	65501
F11—C34	3.49(1)	54501	O12—C22	3.58(1)	57402
F12—C23	3.41(1)	56402	O13—C43	3.36(1)	57502
F12—O22	3.44(1)	57402	O13—C34	3.41(1)	54501
F12—C24	3.52(1)	56402	O13—C44	3.44(1)	57502
F13—O23	3.019(9)	57402	O22—C24	3.37(1)	56501
F13—C33	3.31(1)	47402	O22—C13	3.41(1)	57502
F13—F21	3.35(1)	57402	O23—C33	3.35(1)	45501
F22—C23	3.23(1)	47402	O23—C32	3.38(1)	45501
F23—C25	3.42(1)	56501			

[a] The ADC (atom designator Code) specifies the position of the latter atom in a crystal.

solvents) with a solution of the anion of interest, monitoring the titration by absorption spectroscopy, or, when precipitates formed, by visual observation. In a few instances, this approach was vitiated by side reactions, but in the majority an end point at ~2.0 mol of nucleophile/mol of V(II) was observed.

The conclusions on the composition of the dominant forms in solutions are bolstered also by the internal consistency of the various items of evidence. For example, where, as in the series VPy_4X_2, X^- being Cl^-, Br^-, or I^-, the differences in absorption spectra are monotonic and gradual, this is strong support for the conclusion that all the halides occupy positions in the coordination sphere. Or, once it is shown that vanadium(II) bromide in pyridine exists as VPy_4Br_2, it is entirely reasonable to suppose that when the counterion is the much stronger nucleophile CH_3O^-, the solute species at 2:1 ratio of this anion to V(II), at an end point, will be $VPy_4(OCH_3)_2$.

In scanning the data from the absorption spectra of tetrapyridine compounds dissolved in pyridine, we see that in almost every case the formula of the dominant form of V(II) in solution corresponds to that implied by the formula entered under the heading "compound". The exceptions occur with the weakest nucleophiles, PF_6^- and BPh_4^-, and these are given separate discussion.

The most prominent feature of the spectra is a band envelope with extinction coefficient at the maximum in excess of 1.0×10^3 M^{-1} cm^{-1}. The main peak is accompanied by a shoulder, usually on the low-energy side, and in such cases the maximum is assigned to MLCT absorption (ν_{CT}) and the shoulder to the higher energy component, ν_1'', of the two transitions which arise from ν_1 in octahedral symmetry when the symmetry is reduced to axial. The cases in which the shoulder lies on the high-energy side of the maximum are dealt with in the Discussion. The enhancement of ϵ for this transition as compared to that of ν_1 or of the lower energy component ν_1' has already been noted.[1,2] In most cases, in pyridine solution it has been difficult to locate ν_1' because, being of low intensity, it is often masked by the wings of bands of much higher intensity at shorter wavelengths. This interference is much reduced in CH_2Cl_2, and in this solvent the long-wavelength absorption is sometimes sufficiently well resolved so that approximate values of the properties of ν_1' were obtained as recorded in Table 6. The spectra for the Cl^-, Br^-, I^-, $CF_3SO_3^-$, and BH_4^- complexes in the long-wavelength region are shown in Figure 2.

Since $CF_3SO_3^-$ was widely used as a weak nucleophile, the speciation of $VPy_4(O_3SCF_3)_2$ (i.e. the nature of the $VPy_4(O_3SCF_3)_2$ species in solution) is of particular importance. Because substitution can be rather facile, there is no assurance that when a solid of composition $VPy_4(O_3SCF_3)_2$ is dissolved in pyridine, the dominant form in solution will have the same composition. But that this is in fact the case is suggested by the observations that Beer's law is obeyed by the salt both in pyridine (0.10×10^{-3} to 0.9×10^{-2} M) and in CH_2Cl_2 (0.30×10^{-3} to 1.0×10^{-2} M) and, of greater consequence, that the general features of the spectra are the same in the two solvents. In order of increasing nucleophilicity, I^- is probably next in line. The compound VPy_4I_2 was found to obey Beer's law in pyridine (1.0×10^{-3} to 1.2×10^{-2} M), but of greater weight are the following observations: the absorption characteristics are different from those of solutions of $VPy_4(O_3SCF_3)_2$ and of $VPy_6(PF_6)_2$ and show a monotonous trend in comparison to those of the Cl^- and Br^- complexes. We conclude that in pyridine it exists as VPy_4I_2 rather than as VPy_6^{2+} or VPy_5I^+.

Except for BPh_4^- and PF_6^-, all the anions used in our studies are stronger nucleophiles than $CF_3SO_3^-$ or I^-, and it is therefore entirely likely that in pyridine each stronger nucleophile in Table 6 also occupies two coordination positions on V(II). A possible exception may be BH_4^-, its ranking as a nucleophile toward V(II), or to other dipositive ions, not being known. Because of the instability (vide infra) of $VPy_4(BH_4)_2$ in pyridine, our attempts at characterization are limited to CH_2Cl_2 (CD_2Cl_2) as a solvent in which decomposition is very slow. Because of the weak nucleophilic character of this solvent, it is likely that the spectrum we recorded for the complex in solution corresponds to the formula given. It is interesting that although V(II) is paramagnetic (high-spin πd^3), good ^1H NMR spectra can be obtained for ligands bound to it.[7a] Some ^1H NMR measurements for $VPy_4(BH_4)_2$ dissolved in CD_2Cl_2 were made. Not surprisingly, the signals for pyridine bound to V(II) integrated

Table 6. UV−Vis and Electrochemical Data for $VPy_4(X)_2$ Complexes in Pyridine and Dichloromethane

entry	compound	soln species (pyridine)	λ, nm ($10^{-3}\epsilon$, M^{-1} cm^{-1})[a]	$E_{1/2}$, V (or E_{pa}, V)[b]
1	$VPy_4(PF_6)_2$		578 (0.22); 440 sh; 400 (5.5) (t_0)[c]	1.03
		VPy_6^{2+}	598 sh; 478 sh; 430 (5.5) (t_f)[c]	0.63
2	$VPy_5(PF_6)_2$	VPy_6^{2+}	598 sh; 478 sh; 430 (5.6)	
3	$VPy_6(PF_6)_2$		598 sh; 478 sh; 430 (5.5)	0.63
4	$VPy_4(BPh_4)_2 \cdot 2Py$[d]		580 (0.2); 440 sh; 400 (5.4) (t_0)[c]	1.03
		VPy_6^{2+}	618 sh; 480 sh; 430 (5.2) (t_f)[c]	0.63
			[580 (0.14); 436 sh; 394 (5.6)]	
5	$VPy_6(BPh_4)_2$[d]		618 sh; 480 sh; 430 (5.3)	0.63
			[610 sh; 460 sh; 410 (5.9)]	
6	$VPy_4(O_3SCF_3)_2$		490 sh; 424 (4.8)	0.67 (100)
			[740 (0.015); 492 sh; 424 (4.6)]	[0.6 (140)]
7	$VPy_4(Cl)_2$		536 sh; 482 (6.7)	−0.06 (80)
			[754;[e] 545 sh; 472 (6.3)]	[−0.05 (120)]
8	$VPy_4(Br)_2$		526 sh; 470 (4.8)	0.15 (90)
			[840 (0.017); 532 sh; 460 (5.4)]	
9	$VPy_4(I)_2$		512 sh; 442 (4.2)	0.27 (90)
			[960 (0.016); 518 sh; 442 (5.5)]	
10	$VPy_4(SCN)_2$		494 (4.5); 456 sh	0.19 (140)
			[492 (3.3); 452 sh]	
11	$VPy_4(N_3)_2$		680 sh; 532 (3.6); 480 sh	−0.29 (70)
12	$VPy_4(SPh)_2$		560 sh; 502 (5.9)	−0.33
13	$VPy_4(BH_4)_2 \cdot CH_2Cl_2$	$VPy_4(BH_4)_2$[f]	[980 (0.18); 730 sh; 532 sh; 452 (3.6); 300 sh]	[−0.05 (100)]
14	$VPy_4(SEt)_2$		576 (2.0); 516 sh	−0.42
15		$VPy_4(OPh)_2$	640 sh; 565 (0.78)	−0.45
16		$VPy_4(OH)_2$	694 sh; 564 (0.50)	−0.33; 0.01
17		$VPy_4(OMe)_2$	708 sh; 586 (1.5)	−0.56; 0.35
18		$VPy_4(Ph)_2$	630 sh; 545 sh; 480 (2.8)	−0.07 (90)
19		$VPy_4(CN)_2$	580 sh; 500 (5.4); 440 sh	0.37
20		$VPy_4(AlH_4)_2$	660 sh; 526 sh; 482 (2.2)	0.08 (100)
21		$VPy_4(H)_2$	690 sh; 565 (2.4); 446 sh	−0.42 (260); 0.79
22	$V(4\text{-}EtPy)_4(O_3SCF_3)_2$		[760 (0.012); 480 sh; 420 (4.96)]	[0.50 (90)]
23	$V(4\text{-}EtPy)_4(Cl)_2$		[780 (0.082); 528 sh; 468 (6.1)]	[−0.17 (80)]
24	$V(4\text{-}EtPy)_4(I)_2$		[992 (0.016); 508 sh; 442 (6.4)]	[0.45]
25		$V(4\text{-}EtPy)_4(Me)_2$[g]	540 sh; 460 (0.98)	
26		$V(4\text{-}EtPy)_4(Et)_2$[g]	530 sh; 455 (1.05)	
27	$V(4\text{-}EtPy)_4(BH_4)_2$		[1000 (11); 760 sh; 534 sh; 468 (2.6); 300 sh]	[−0.15 (80)]
28	V(ethyl isonicotinate)$_4(O_3SCF_3)_2$		[518 (4.6); 476 (4.8); 300 sh]	[0.94 (160)]

[a] Entries in brackets pertain to solutions of the solids in CH_2Cl_2. [b] Where $E_{1/2}$ is given, this is followed by ΔE_p in parentheses; otherwise E_{pa}. Unless otherwise stated electrolyte is $[^tBu_4N]PF_6$. [c] t_0, measurements made immediately after dissolving; t_f, measurements made at conclusion of reaction. [d] $[^tBu_4N]BPh_4$ as electrolyte. [e] Value estimated by using the average difference between the pyridine and 4-substituted pyridine derivatives noted for the $CF_3SO_3^-$ and I^- complexes. [f] In CH_2Cl_2. [g] Species of entry 25 was characterized in Et_2O, and that of entry 26 in THF.

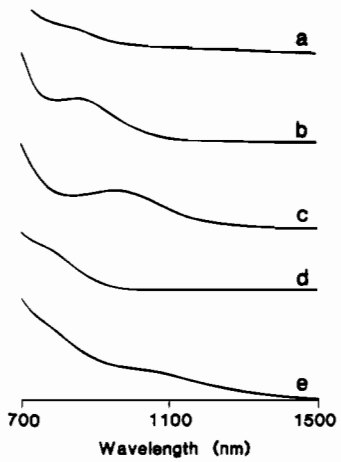

Figure 2. Low-energy absorption spectra (ν_1') collected in CH_2Cl_2: (a) $V(4\text{-}EtPy)_4Cl_2$; (b) VPy_4Br_2; (c) VPy_4I_2; (d) $VPy_4(CF_3SO_3)_2$; (e) $VPy_4(BH_4)_2$.

to the expected number, but because the signal for free pyridine, as determined in a separate experiment, is indistinguishable from that of bound pyridine, the experiment failed in its purpose. That free BH_4^- does not survive in CH_2Cl_2 coupled with the fact that a single signal for ^1H in BH_4^- is observed shows that BH_4^- is firmly bound and that rotation is rapid on the ^1H NMR time scale.

For entries 6−14, we conclude that the constitution of the complex in the solid is retained in solution. The electrochemical measurements add little to the evidence on speciation, but the data themselves require some comment. It is reassuring that, in the two cases, namely $CF_3SO_3^-$ and Cl^- complexes, in which measurements in CH_2Cl_2 were also made, the electrochemical data obtained in the two media agree.

A problem in interpreting the electrochemical results arises in the case of weak nucleophiles; because a high concentration of electrolyte must be used to provide conductance, it is possible that the anion of the supporting electrolyte changes the nature of the species. The salt $[^tBu_4N]PF_6$ was chosen as electrolyte because PF_6^- is presumed to be one of the weakest nucleophiles dealt with. There is no reason to believe that the background electrolyte affected the speciation except possibly in the cases of the $CF_3SO_3^-$ and BPh_4^- complexes. The complications observed for $VPy_4(O_3SCF_3)_2$ are described herewith. With $[^tBu_4N]PF_6$ as supporting electrolyte, $E_{1/2} = 0.67$ V is observed (but with E_{pc} less developed than E_{pa}), as is also a stronger signal, $E_{pa} = 0.94$ V. With $[^tBu_4N]O_3SCF_3$ as supporting electrolyte, the peak positions are not altered, but now the signal at 0.67 V is much stronger than that at higher potential. By the use of VPy_4Cl_2 as an internal standard and with $[^tBu_4N]O_3SCF_3$ as supporting electrolyte, we find that the signals at 0.67 and 0.94 V must be combined to account for a $1e^-$ change (Figure 3). In the experiment, in addition to the signal expected for VPy_4Cl_2 ($E_{1/2} = -0.06$ V), a small signal is observed at

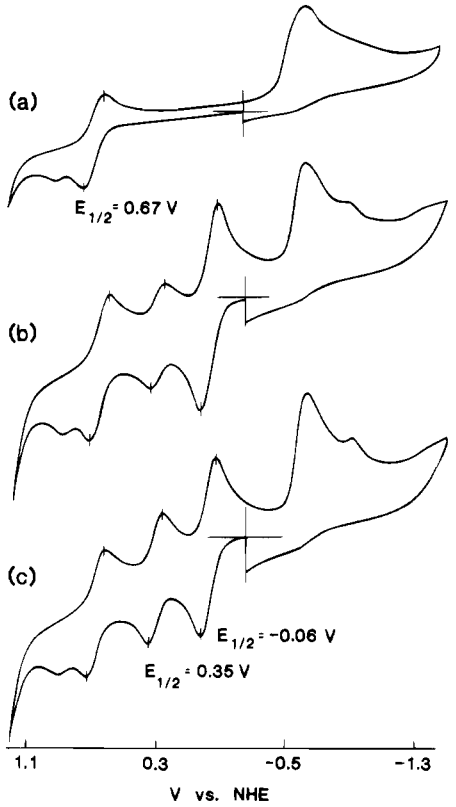

Figure 3. (a) CV of $VPy_4(CF_3SO_3)_2$ (2.3×10^{-3} M and in 0.1 M TBAOTf) in pyridine solvent. (b) CV of the sample in (a) with VPy_4Cl_2 (1.96×10^{-3} M) taken after 5 min of mixing. (c) CV of the sample in (b) after 2 h.

$E_{1/2} = 0.35$ V, which we ascribe to $VPy_4(O_3SCF_3)Cl$. Because of the agreement between the values of $E_{1/2}$ measured for $VPy_4(O_3SCF_3)_2$ dissolved in pyridine and in CH_2Cl_2, we attribute the signal $E_{1/2} = 0.67$ V to the $VPy_4(O_3SCF_3)_2^{+/0}$ couple and leave for later comment the origin of E_{pc} at higher potential. For most of entries 6−11 and 13, the product of the $1e^-$ oxidation lasts long enough so that the amplitudes of E_{pa} and E_{pc} match even at a sweep rate of 100 mV s^{-1}, but for the NCS^- complex the condition is met only at higher scan rates, up to 2 V s^{-1}. With PhS^- and EtS^- (entries 12 and 14) well-defined anodic waves are observed, but the complementary cathodic waves did not appear, even at highest scan rates. In these cases, electron loss is presumably followed by a rapid rearrangement of the product.

In pyridine as solvent, with the exception of $VPy_4(N_3)_2$ and VPy_4Ph_2 as solutes, reduction waves are observed in the range −0.4 to −0.8 V, but only after the oxidation of V(II) to V(III) has occurred. Specifically, no action is observed in this potential range when a scan starting at −0.3 V is made to more negative potentials, but it does occur when the scan, again starting at −0.3 V, is first made to positive potentials and is reversed after $E_{1/2}$ (or E_{pa}) corresponding to V(II) → V(III) is registered. The amplitudes can be high, in some cases exceeding by a factor of 3 or 4 that corresponding to a $1e^-$ change, and for some complexes, more than one wave is observed (see Figure 3 for CV of **1**). For VPy_4Cl_2 as solute, we found that the reduction wave in question, which appears at −0.45 V at a scan rate 100 mV s^{-1}, disappears when the scan rate is increased to 2 V s^{-1}. At high scan rates, V(III), as first formed, is completely reduced to V(II)(E_{pc} and E_{pa} match in amplitude), suggesting that only V(III) which has undergone irreversible substitution is involved in the appearance of the high-amplitude waves.

The remaining tetrapyridine complexes were prepared by the titration procedure. For most of them, there is little reason to doubt that the species are those represented in the second column of Table 6. With the use of LiOH, $LiOCH_3$, and LiPh in titration, stepwise addition of the salts to a solution containing $VPy_4(O_3SCF_3)_2$ shows progressive changes in the spectrum and the solutions remain homogeneous until the 2:1 ratio is reached, after which black precipitates form. Black precipitates also form when diethyl ether is added to a solution titrated to the 2:1 ratio. As to the solutions themselves, when they are dilute, ca. 1×10^{-3} M, they are stable for hours.

Of the species prepared by titration, VPy_4Ph_2 is the most stable, and it persists for a period of a month without apparent decomposition when the solution is stored at −20 °C. In the course of doing electrochemical measurements, we noted that a 2.2×10^{-3} M solution of VPy_4Ph_2 in pyridine which contained $[^tBu_4N]O_3SCF_3$ as supporting electrolyte showed no noticeable decline in the reversible signal after being kept at room temperature for 12 h. Cyclic voltammetric measurements during titration showed that, at an intermediate stage, a signal appears at $E_{1/2} = 0.27$ V. The signal for $VPy_4(O_3SCF_3)_2$ disappears when the ratio of Ph^- to V(II) slightly exceeds 2:1, and we see only the signal $E_{1/2} = -0.07$ V, which assign to VPy_4Ph_2. On the basis of these observations, the signal at $E_{1/2} = 0.27$ V, intermediate between +0.67 and −0.07 can reasonably be assigned to $VPy_4Ph(O_3SCF_3)$. With LiOPh and LiSPh as titrants acting on $VPy_4(O_3SCF_3)_2$ (ca. 1.0×10^{-2} M), precipitates do not appear even when the salts are added in some excess. Instead, the absorption reached in the visible region of the spectrum at the 2:1 ratio remains unchanged, but a slight increase in the high-energy region is noted even beyond the end point.

In the preparation of the CN^- complex, $[^tBu_4N]CN$ was used as the titrant. When this is added to a level of 2.5 mol/mol of $Vpy_4(O_3SCF_3)_2$ (1.0×10^{-3} M), a break in the absorption is observed slightly beond the 2:1 ratio. In this system, the end point is not as well defined as it is in most of the others. The cyclic voltammetry on a solution prepared in this way shows only a single oxidation wave in the range +1.4 to −1.4 V, indicating that mainly a single component is present. The absorption and electrochemical characteristics of the solution are unaltered even after it is kept at room temperature for 12 h. Changes in absorption continue on addition of the titrant beyond the 2:1 ratio, and it appears that CN^- can rather readily replace pyridine from V(II). When diethyl ether is added to a solution titrated to the 2:1 ratio, a dark red solid precipitates which does not dissolve in pyridine. Bridging by CN^- can account for the insolubility of the dark red solid.

The complex which we believe is $VPy_4(AlH_4)_2$ was obtained in the course of attempting to prepare a dihydrido species. The addition of LiH to $VPy_4(O_3SCF_3)_2$ in pyridine results in a black solid. However by use of a solution of $LiAlH_4$ in Et_2O (1.0 M), decomposition can be controlled. Successive portions were added to a solution of $VPy_4(O_3SCF_3)_2$ in pyridine (1.6×10^{-4} M) precooled to −10 °C prior to the addition; each portion provided 0.50 mol of $LiAlH_4$/mol of V(II). The changes, appearance of absorption at lower energy at the expense of that characteristic of $VPy_4(O_3SCF_3)_2$, take place with a half-life of 1 or 2 h as the solution warms to room temperature. After each 12 h interval, another aliquot was added, the maximum in the new absorption being reached after the addition of the fourth aliquot. The end point corresponds to approximately 2 mol of $LiAlH_4$/mol of V(II). The data recorded in Table 6 are those obtained for this solution. On the addition of more $LiAlH_4$, the new absorption decreases in intensity, though the general shape of the band remains unchanged. While the reaction

$$VPy_4^{2+} + 2LiAlH_4 + 2Py = VPy_4H_2 + 2Py{\cdot}AlH_3 + 2Li^+$$

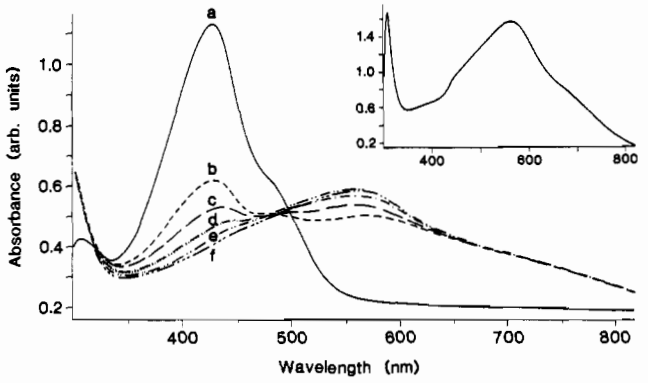

Figure 4. Overall UV−vis absorbance changes in the formation of VPy_4H_2 from $VPy_4(CF_3SO_3)_2$ in pyridine solvent: (a) spectrum of $V(Py)_4(CF_3SO_3)_2$ at room temperature; (b) spectrum of the sample in (a) with $LiEt_3BH$ (H^-/V(II) ratio = 2.2; overnight reaction) at −20 °C; (c−f) spectra recorded within 6 min while the solution from (b) warms to room temperature. The inset shows the optimum spectrum for $VPy_4(H)_2$.

conforms to the 2:1 stoichiometry, on the basis of results now to be described, this is unlikely.

By the use of a monohydride, $LiEt_3BH$ (Super Hydride), a product is obtained with properties quite different from those we attribute to the bis tetrahydrido species. When a solution of $VPy_4(O_3SCF_3)_2$ in pyridine (2.3×10^{-3} M) at −20 °C is treated with enough Super Hydride to bring the H^-:V(II) ratio to 2.2, the spectrophotometric responses shown in Figure 4 are registered. When the solution is kept overnight at −20 °C, the reaction, as judged by the decrease in absorption of $VPy_4(O_3SCF_3)_2$, is somewhat more than 50% complete. When the solution is allowed to warm to room temperature, the changes are much more rapid, necessitating measurements to be made at intervals of a few minutes. The product has λ_{max} at 565 nm and a shoulder at 690 nm (see Table 6), the band intensity reaching a maximum and then decreasing. The solution containing what we believe is the dihydride is purple, as contrasted with a solution of what we believe is $VPy_4(AlH_4)_2$, which is wine red.

When the same procedure is followed in THF as solvent, as in the previous case, a stage is reached at which $VPy_4(O_3SCF_3)_2$ has been consumed, and the purple color reaches a maximum. The features of the spectrum are like those recorded in Table 6 for the dihydride, except that the high-energy shoulder appears at somewhat longer wavelength. The stability of the dihydride in THF at room temperature however is no greater than it is in pyridine.

Early attempts to prepare a dihydride at room temperature by the reaction of $LiBH_4$ with $VPy_4(O_3SCF_3)_2$ at (2:1 ratio) in pyridine led to purple solutions after a very short reaction time, but also to rapid disappearance of the color. However, by following the procedure described using Super Hydride, we obtained a product with spectrophotometric properties almost identical to those just cited (λ_{max} = 565 nm; $\epsilon = 2.4 \times 10^3$ cm^{-1}). As in the case of the Super Hydride as reagent, substitution at −20 °C is extremely slow, only ca. 25% of the starting material being consumed in 12 h. However, upon removal of the cuvette from the cold to record the spectrophotometric measurements, the maximum absorption at 565 nm is reached after 5 min, and 5 min later it declines 5%. The extinction coefficient measured at the maximum is 2.4×10^3 M^{-1} cm^{-1}.

A solution containing the purple species was prepared by following the first procedure, but with the difference that after the reaction mixture was removed from the cold, it was kept at

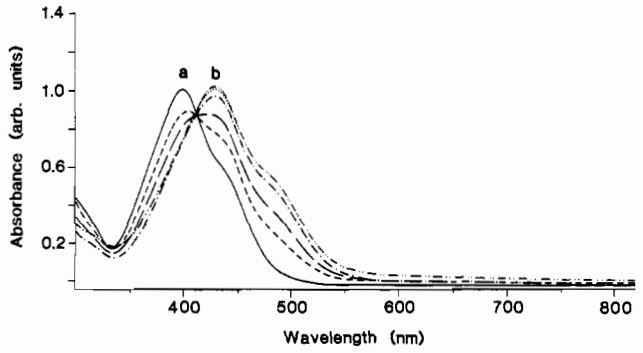

Figure 5. (a) UV−vis absorption spectra of $VPy_4(PF_6)_2$ in pyridine at −20 °C. (b) Final spectrum of the sample in (a) reached after ~30 min upon warming to room temperature.

room temperature for 15 min and then cooled rapidly. Electrolyte was added to facilitate the electrochemical measurements, and these were carried out with the solution kept at −20 °C. A reversible signal is observed with E_{pa} and E_{pc} at essentially equal amplitude, when the sweep to higher potential is started at −0.70 V. In fact, if the sweep is started at 0.0 V, a potential positive of $E_{1/2}$, and carried to negative potentials, the same response is observed as in starting at negative potentials. The amplitudes observed for $E_{1/2}$ correspond to $1e^-$ changes while the irreversible wave at E_{pa} = 0.79 V (see Table 6) is of greater amplitude. In the present system, the unexplained feature at negative potentials, which frequently appears after the oxidation pulse, is very prominent. We believe that $E_{1/2}$ = −0.42 V applies to the $VPy_4H_2^{+/0}$ couple, but the interpretation of E_{pa} = 0.79 V is not certain. Its appearance does not affect $E_{1/2}$, and it is possible that BEt_3, which is a product of the reaction, is being oxidized.

The facts that the same substance was prepared by use of Super Hydride and of $LiBH_4$, that the spectrophotometric properties are quite different from those of $VPy_4(BH_4)_2$, that the electrochemical properties are also different, and that the stoichiometry of the reaction with Super Hydride is 2:1 make it substantially certain that we have in hand VPy_4H_2, a novel species.

The interpretations of the solution properties of the solids prepared with PF_6^- and BPh_4^-, the weakest nucleophiles, are less straightforward than in the other cases, and on this account, their consideration has been deferred. In the preparation section, it is noted that, depending on the length of time the mixture of $V(MeCN)_6(PF_6)_2$ in pyridine is stirred, different compositions result: $VPy_4(PF_6)_2$, when the time is short, and $VPy_6(PF_6)_2$, when it is long. To obtain the spectrum characteristic of the tetrapyridine compound, it was taken in pyridine at −20 °C. The maximum appears at ~400 nm, and when the solution warms to room temperature, this shifts to 430 nm within 30 min, the wavelength of the maximum when the hexapyridine salt is dissolved. We conclude that when $VPy_4(PF_6)_2$ is dissolved, we initially record its spectrum, and it is then transformed to VPy_6^{2+}. The transformation of $VPy_4(PF_6)_2$ to the ultimate product gives rise to an isosbestic point (see Figure 5). This implies that in the substitution an intermediate stage does not accumulate in substantial concentration—that is, substitution on $[VPy_5(PF_6)]^+$ must be more rapid than that on $VPy_4(PF_6)_2$. This is borne out by the fact that when $VPy_5(PF_6)_2$ is dissolved, even at −20 °C the first spectrum taken corresponds to that of VPy_6^{2+}. Beer's law is obeyed by the solution prepared from $VPy_6(PF_6)_2$ as well as by the solution which contains the ultimate product of the dissolution of $VPy_4(PF_6)_2$.

The measurements with $VPy_4(BPh_4)_2 \cdot 2Py$ were carried out in the same way as those described for $VPy_4(PF_6)_2$. The changes on dissolution take place on the same time scale as for the PF_6^-

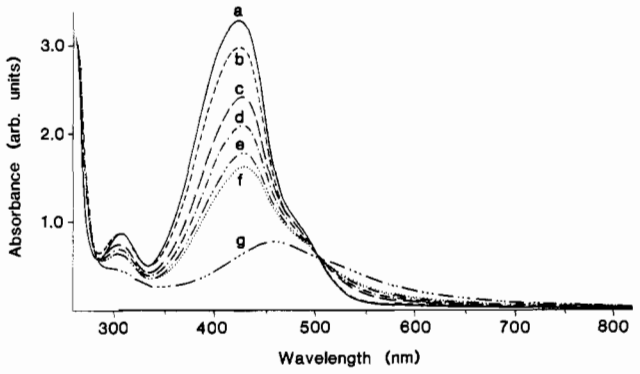

Figure 6. Absorption measurements vs time for the $V(4\text{-}EtPy)_4(CF_3SO_3)_2$–LiMe system in Et_2O at 25 °C: (a) spectrum before addition of LiMe; (b–g) spectral changes recorded over a period of 12 h after the addition of the reagent.

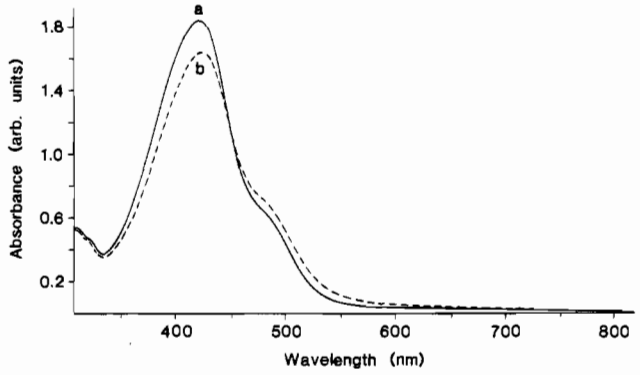

Figure 7. (a) Absorption spectrum of $VPy_4(CF_3SO_3)_2$ in pyridine. (b) Spectrum of the sample in (a) in the presence of 100 mol of H_2O/mol of V(II) (immediate response).

salts, and as before, an isosbestic point is observed. The final spectrum corresponds to that we have assigned to VPy_6^{2+} when PF_6^- is the counterion. Spectrophotometric measurements on the two BPh_4^- salts were made also in CH_2Cl_2 as solvent, but they add little in the way of evidence. Though absorption characteristics we assign to VPy_6^{2+} are somewhat different for the two media, the differences can be ascribed to the change in solvent (compare with data for entries 7 and 8, for example). It should be noted that the overall compositions of the solutions of the two BH_4^- salts in CH_2Cl_2 are the same, but the resulting spectra are different and remain so, showing that equilibration in CH_2Cl_2 is *very* slow.

The electrochemical measurements support the conclusions which have been reached about the nature of the species in solution. Those for $VPy_4(PF_6)_2$ and $VPy_4(BPh_4)_2 \cdot 2Py$ as solutes were made at −20 °C. The initial values are entered in Table 6 as $E_{pa} = 1.03$ V. They differ markedly from the final values, which at $E_{pa} = 0.63$ V agree, and agree also with those obtained for solutions of $VPy_6(PF_6)_2$ and $VPy_6(BPh_4)_2$. The fact that the values of E_{pa} for newly made solutions of the solutes of entries 1 and 4 must be attributed to coincidence.

While the main reason for resorting to the ethyl derivative of pyridine was to minimize the possibility of deprotonation of pyridine by the strong nucleophiles (entries 25 and 26), four additional compounds were prepared for the purpose of comparisons to be made later. The results obtained with the solids in solution appear under entries 22–24 and 27 in Table 6 and are consistent with those obtained with the corresponding tetrapyridine species. The only novel results are those for CH_3^- and $C_2H_5^-$ as nucleophiles. Those from the reaction with $LiCH_3$ are reported in greater detail because the reaction course is rather unusual. A solution of $LiCH_3$ in Et_2O (1.1 M) was added to $V(4\text{-}EtPy)_4(O_3SCF_3)_2$ dissolved in Et_2O, raising the ratio of CH_3^- to V^{2+} to slightly in excess of 2:1, and the absorbance was followed as a function of time (see Figure 6) at room temperature. The fact that an isosbestic point is obtained indicates that the reaction is free of major side products and that reaction occurs with only minor accumulations of $VPy_4(O_3SCF_3)(CH_3)$. At the 2:1 ratio of the solutes, the product remains unchanged when the reaction solution is kept for 12 h. The 2:1 ratio is an end point; at this ratio, the original V(II) species has been consumed, and excess $LiCH_3$ leads to a decrease in the concentration of $VPy_4(CH_3)_2$.

The preparation of the ethylide derivative was conducted along the lines described. In this case however, the reaction is stepwise. Though, with $C_2H_5^-$ as ligand, β-elimination is a possibility, that is obviously not a factor in the reaction system, because the absorption properties are very different from those recorded for the dihydride but similar to those of the methylide and because it shows similar stability.

Some experiments were also done to study the effect of neutral ligands on $VPy_4(O_3SCF_3)_2$ as the solute in pyridine. Among them, the most important for our purposes is water. Pyridine is notably difficult to dry, and there is always concern about the effect of residual water on the observations. In a series of experiments with V(II) at 5.6×10^{-4} M, on the addition of 6×10^{-2} M H_2O, λ_{max} moves from 424 to 428 nm and ϵ decreases from 4.6×10^3 to 3.6×10^{-3} M^{-1} cm^{-1}. Moreover, while ϵ at the band maximum decreases, that at the shoulder increases (see Figure 7). The same changes are brought about also by the addition of 2.8×10^{-3} M H_2O. These changes are complete in the time, ca. 5 min, which is needed to record the spectrum. Moreover, an increase to 0.30 M H_2O does not significantly alter the response in the absorption spectra at least on a short time scale. With the higher concentrations of water, additional changes do take place slowly ($t_{1/2}$ at least 30 min), which, with enough water, can lead to large decreases in the absorbance and slight shifts to longer wavelength. The biphasic behavior shows that sequential events are occurring. While the first stage might be ascribed to replacement of $CF_3SO_3^-$ by water, this is rendered unlikely by the results of experiments, in which attempts made (vide infra) to bind imidazole to V(II) in pyridine proved futile even though it is a much stronger nucleophile than water. It is also difficult to explain the results of the electrochemical experiments on this basis. These experiments were done with a solution of $VPy_4(O_3SCF_3)_2$ in pyridine to which water had been added (13 mol/mol of V(II)). The measurements were made soon after mixing to avoid complications resulting from the progress of the second slow reaction phase. For $VPy_4(O_3SCF_3)_2$ ($[^tBu_4N]CF_3SO_3$ as electrolyte) at 100 mV s^{-1} scan rate, E_{pa} is observed at 0.70 V but the wave is quite indistinct, and a faint signal appears at $E_{pa} \sim 0.94$. At a scan rate of 1 V s^{-1}, E_{pc} complementary to E_{pa} at 0.70 V appears, leading to $E_{1/2} = 0.67$, identical to that observed without added water.

The immediate effect of water may be that it modifies the nature of the anionic ligand by hydrogen bonding to oxygen. The effect of association with water may be canceled in the electrochemical experiments because it will affect both oxidation states.

For VPy_4Cl_2 dissolved in pyridine there was no change in the major absorption band or the shoulder on the addition of 50 mol of H_2O/mol of V(II), even after 2 h. No change in the spectrum of $VPy_4(O_3SCF_3)_2$ in pyridine was observed with *N*-methylimidazole, at 1.6×10^{-3} M (about the same concentration as the lowest level of H_2O), even after 12 h. On the addition of PMe_3 (3.8×10^{-2} M) to a solution of $VPy_4(O_3SCF_3)_2$ in

Table 7. UV−Vis and Electrochemical Results for V(II)−Acetonitrile Complexes in Acetonitrile

entry	compound	λ, nm ($10^{-3}\epsilon$, M^{-1} cm^{-1})	E_{pa}, V
1	$V(MeCN)_6(BPh_4)_2$	614 (0.051); 446 (0.047); 284 sh; 240 (11.4)	*a*
2	$V(MeCN)_6(O_3SCF_3)_2$	614 (0.054); 446 (0.049); 284 sh; 240 (11.3)	1.34
3	$V(MeCN)_4Cl_2$	682 (0.042); 490 (0.06); 282 (21.8)	0.63
4	$V(MeCN)_4Br_2$	658 (0.042); 480 (0.06); 420 sh; 250 (7.6); 220[b] (18.0)	0.86

[a] Due to interference by oxidation of the BPh_4^- ion, definite assignment of the oxidation potential of the V(II)/V(III) couple could not be made. [b] $\pi-\pi^*$ intraligand transition of the bromide ion.

tetrahydrofuran (1.9×10^{-2} M), again no change in the spectrum was observed, and the solid recovered proved to be identical to the starting material. The experiments just described suggest that replacement of anions from V(II) by residual water in the pyridine is not a serious issue in any of the systems.

In the interest of completeness, some complications in the electrochemical results need to be mentioned. With the halides, additional waves (E_{pa}) in the high-potential region (Br^-, 1.2 V; I^-, 0.5 V) are observed which are ascribable to oxidation of the ligands. This we believe is also the origin of additional waves which appear for NCS^-, PhS^-, and EtS^- complexes (E_{pa} = 0.9, 0.3, and 0.2 V, respectively). Extra waves are also observed for PhO^-, CH_3O^-, and HO^- at E_{pa} = 0.5, 0.35, and 0.005 V, respectively. In view of the great nucleophilic power of the ligands, which stabilizes the V(III) state relative to V(II), these are too positive to be attributable to the mononuclear complexes but they are not positive enough to be assigned to ligand oxidation. It is known that $V(OH)^{2+}$ species condense to binuclear forms,[2,8a] and it is likely that $V(OCH_3)^{2+}$ and $V(OPh)^{2+}$ behave similarly. Oxidation of such binuclear species has been reported.[24]

Chemistry in Acetonitrile Solution. The data obtained in the study of the speciation of V(II) in acetonitrile in the presence of a variety of anions are summarized in Table 7.

The preparation of $V(CH_3CN)_4Cl_2$ by dissolving $VCl_2 \cdot 2CH_3OH$ in acetonitrile has been reported.[4] The use of $V(CH_3CN)_6(O_3SCF_3)_2$ as the source of V(II) provides another method for the preparation of tetraacetonitrile complexes. Observations which are described below show that when $CF_3SO_3^-$ is the counterion, V(II) in CH_3CN exists as $V(CH_3CN)_6^{2+}$. Since $CF_3SO_3^-$ does not displace CH_3CN from the coordination sphere, it offers no competition for the entry of other nucleophiles.

In the preparation of $V(CH_3CN)_6(BPh_4)_2$, silver carbonate was added in slight excess (mole ratio 2.3) to a mixture of 0.98 mmol of $V(CH_3CN)_4Cl_2$ in 10 mL of CH_3CN (the salt is not completely soluble). The liquid was stirred for 18 h at room temperature, whereupon the precipitate was removed by filtration. The resulting green solution, where the anion now is CO_3^{2-}, appeared to be identical to that of $V(CH_3CN)_6(O_3SCF_3)_2$ dissolved in CH_3CN. The measurement of the absorption spectrum showed maxima at 446 and 614 nm ($\epsilon \sim 48$ and 53 M^{-1} cm^{-1}), respectively, characteristics almost identical to those recorded for a solution of the triflate salt. (It is a point of interest that CO_3^{2-} as a counterion does not cause precipitation of a V(II) salt in CH_3CN; it is even more remarkable that CO_3^{2-} does not displace CH_3CN from the coordination sphere of $V(CH_3CN)_6^{2+}$.) On the addition of $NaBPh_4$ (ratio 2.5:1), a white precipitate formed which we take to be Na_2CO_3. This was removed by filtration. The spectrum of the solution, in which BPh_4^- is now the counterion, is also at this stage identical to that recorded for the triflate salt dissolved in acetonitrile.

Thus we have found the spectra of solutions of V(II) in acetonitrile with $CF_3SO_3^-$, CO_3^{2-}, and BPh_4^- as counterions to be the same. In view of the sensitivity of the absorption spectra to the nature of other nucleophiles, the only reasonable interpretation is that a common form $V(CH_3CN)_6^{2+}$ is present in the three environments.

On the addition of LiCl to a solution (6.7×10^{-3} M) of $V(CH_3CN)_6(O_3SCF_3)_2$ in CH_3CN, when the end point at the 2:1 ratio is reached, the spectrum changes to that observed on dissolving $V(CH_3CN)_4Cl_2$ in CH_3CN. Similar observations were made for $V(CH_3CN)_4Br_2$, but in this case, [$^tBu_4N$]Br was used as titrant. Although solid $V(CH_3CN)_4Br_2$ was prepared by the addition of LiBr to a solution of $V(CH_3CN)_6(O_3SCF_3)_2$ in CH_3CN, the corresponding iodide salt could not be prepared by this method. Moreover, no change in absorption spectrum follows on addition of LiI to a concentration of 2.0×10^{-2} M and apparently the affinity of I^- for V(II) in CH_3CN is very low.

Attempts to prepare the bis(phenolate) or bis(thiophenolate) species failed. An immediate color change was observed. Upon introduction of either nucleophile, the solution, originally greenish blue, changed to purple and after 15 min turned black. The solid which formed upon following the usual procedures proved not to be completely soluble in acetonitrile.

The results of the electrochemical experiments in acetonitrile also appear in Table 7. In this solvent, in none of the cases was a value of $E_{1/2}$ obtained even at scan rates as high as 2 V s^{-1}. The three values of E_{pa} obtained are distinctly different, and in the case of the Cl^- and Br^- complexes, it is likely that the values of E_{pa} recorded correspond to the tetraacetonitrile complexes. From the electrochemical data alone, no conclusion can be drawn about the speciation of $V(CH_3CN)_6(O_3SCF_3)_2$ in acetonitrile. The electrochemical behavior of VPy_4Cl_2 dissolved in CH_3CN was also investigated. Because the same value of E_{pa} is obtained as that for $V(CH_3CN)_4Cl_2$ in CH_3CN and because the behavior is quite different from that of VPy_4Cl_2 in pyridine, we conclude that VPy_4Cl_2 when it is dissolved in CH_3CN is reorganized to $V(CH_3CN)_4Cl_2$. For the Cl^- and Br^- complexes, in addition to the electrochemical data recorded in the Table 7, E_{pa} values of 1.6 and 1.2 V, respectively, were observed, which we attribute to the oxidation of the coordinated halides.

Complexes of the $V(DMPE)_2(X)_2$ Series. Three compounds of the series, viz. $V(DMPE)_2(Cl)_2$, $V(DMPE)_2(BH_4)_2$, and $V(DMPE)_2(Me)_2$, have been reported, and the crystal structures of the first two have been described.[7] However, no experiments were done to determine the absorption spectra in solution or to determine the redox potentials. Data bearing on these issues for a number of complexes of this class prepared in the course of our work are summarized in Table 8. No complications were encountered, and it appears certain from the nature of our results that the species in solution have the same composition as in solid state.

Discussion

Structure. Long and Clarke reported that a series of complexes of the type MPy_4Cl_2 (M = Fe^{2+}, Co^{2+}, Ni^{2+} all possess orthorhombic (222) symmetry.[25] However, $VPy_4(CF_3SO_3)_2$ shows the "pseudooctahedral" geometry with only C_1 symmetry. The V−O distances of 2.127(6) and 2.129(6) Å in

(24) Money, J. K.; Folting, K.; Huffman, J. C.; Christou, G. *Inorg. Chem.* **1987**, *26*, 944.

(25) Long, G. J.; Clarke, P. J. *Inorg. Chem.* **1978**, *17*, 1394.

Table 8. UV−Vis and Electrochemical Results for $V(DMPE)_2X_2$ Complexes in Dichloromethane

entry	compound	λ, nm ($10^{-3}\epsilon$, M^{-1} cm^{-1})	$E_{1/2}$, V (ΔE_p, mV)
1	$V(DMPE)_2(O_3SCF_3)_2$	712 sh; 626 (0.035); 510 (0.034); 298 (3.1); 266 sh; 244[a] (5.7)	0.83 (E_{pa})
2	$V(DMPE)_2(Cl)_2$	736 (0.011); 520 (0.039); 454 sh; 340 sh; 312 (2.0); 246[a] (6.4)	−0.35 (70)
3	$V(DMPE)_2(Br)_2$	770 (0.010); 512 (0.042); 340 sh; 318 (2.9); 246[a] (8.0)	−0.19 (70)
4	$V(DMPE)_2(I)_2$	818 (0.008); 702 sh; 518 (0.033); 400 sh, 332 sh; 298 sh, 280 (0.99); 255[a] (1.3)	−0.02 (80)
5	$V(DMPE)_2(BH_4)_2$	716 (0.025); 508 (0.063); 346 sh; 302 sh; 274 (4.2); 250[a] (7.8)	−0.28 (100)
6	$V(DMPE)_2(Me)_2$[b]	570 sh; 508 sh; 418 (0.29); 342 sh; 318 (2.9) 265 sh; 246[a] (5.9)	[c]

[a] $\pi-\pi^*$ intraligand transition of the coordinated DMPE ligand. [b] Spectrophotometric data in Et_2O. [c] Due to the reactivity of the solute toward common electrochemical solvents, we tried to obtaine the CV in Et_2O with $Li(O_3SCF_3)$ as a supporting electrolyte, but the conductivity of the solution was so low that we were unable to detect any response.

1 are close to those reported for $V(H_2O)_6(CF_3SO_3)_2$ (2.129 Å),[3e] $V(CH_3COOH)_4Cl_2$ (2.127 Å),[3f] and $V(MeOH)_6Cl_2$ (2.123 Å).[6a] The average V−N distance for the present complex, 2.187 Å, is close to that reported for VPy_4Cl_2 (2.189 Å), and the dihedral angles between VN_4 and pyridine rings (52.7−50.3°) are also close to those reported for VPy_4Cl_2 (51°).[26] The major structural difference between the previously reported vanadium monomers and **1** is the distortion of the two *trans* axial ligands from linearity: in VPy_4Cl_2 the Cl−V−Cl angle is 180° and in $V(CH_3COOH)_4Cl_2$ it is 179.6°, but in **1** the O−V−O angle is 173.5° (Table 2). This large distortion from linearity is uncommon in the first-row transition metal complexes of the type MPy_4X_2. We attribute this to the C--H···X (X = F, O) dipolar[27] or hydrogen bond like interaction[28] because these bond distances are substantially less than those calculated from van der Waals radii. The existence of C--H···X (X = O, N, Cl) hydrogen bonds and their important role in crystal packing and, to some degree, in the molecular conformation of organic molecules (e.g. amino acids and carbohydrates) are being delth with in the current literature[29] but are infrequently referred to in discrete metal coordination complexes.

Spectroscopy. We have in the spectrophotometric studies focused on the low-energy region of the spectra, that showing ν_{CT}, which corresponds to metal to pyridine charge transfer absorption, and ν_1' ($^4B_{1g} \rightarrow {}^4E_g{}^a$) and ν_2'' ($^4B_{1g} \rightarrow {}^4B_{2g}$), the two transitions which in axial symmetry arise from ν_1, the lowest energy absorption for V^{2+} in an octahedral environment. The weak band which arises from $^4B_{1g} \rightarrow {}^4E_g{}^a$ is found to shift to lower energy as the field strength (Dq^z) of the axial ligands decreases; i.e., λ_{max} for ν_1' follows the normal spectrochemical sequence $N_3^- > Cl^- > Br^- > I^-$, as observed for other tetragonal metal complexes.[30] The high-intensity band envelope at higher energy contains ν_{CT}. In most cases, a shoulder appears on the low-energy side of the band maximum, and in these cases, we assign the maximum to ν_{CT} and the shoulder to ν_1''. In some cases, the minor band appears on the high-energy side of the dominant peak, and in these instances, we must deal with

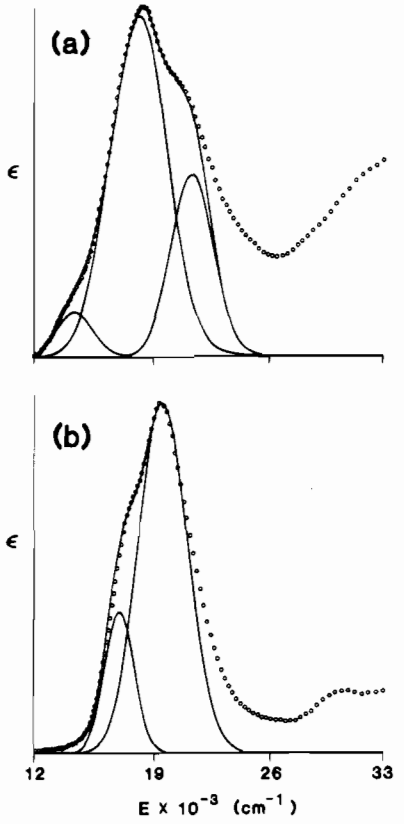

Figure 8. Gaussian resolutions of the room-temperature visible absorption spectra of $VPy_4(N_3)_2$ (top frame) and $VPy_4(Cl)_2$ (bottom frame). The symbols (o) represent the experimental absorption spectra.

the possibility that the shoulder arises from ν_2, which corresponds to the $^4B_{1g} \rightarrow {}^4A_{2g}$ (ν_2') transition. An examination of the absorption spectrum of $VPy_4(CF_3SO_3)_2$ (Figure 7a) where ν_{CT} appears at 424 nm, the highest energy recorded for any of the complexes we have studied, makes this unlikely. It is to be noted that two transitions of similar but rather low intensities appear at 330 and 310 nm. For VPy_4Cl_2, where ν_{CT} appears at 536 nm, two transitions of lower intensity are again observed (ν = 330 and 310 nm), well removed from ν_{CT}. The comparison with $VPy_4(O_3SCF_3)_2$ shows that the energies of these transitions are not very sensitive to the nature of the axial ligands, and we conclude that we can dismiss the intervention of ν_2' (and ν_2'') in the energy region of our interest.

In an earlier publication,[1] the enhancement of ϵ for ν_1'' as compared to the values of ϵ observed when only saturated molecules are ligated was noted, but in the absence of an attempt at deconvolution, the intensities were greatly underestimated. We have carried out the deconvolution in two cases, $VPy_4(N_3)_2$ and VPy_4Cl_2. The results are shown in Figure 8, and they lead to the respective values of $\epsilon(\nu_1'')$ as 1.8×10^3 and 2.7×10^3 M^{-1} cm^{-1}. The assignment of the former may be in doubt (see below), but the latter almost certainly corresponds to ν_1'' and demonstrates an enormous enhancement of the intensity of a d−d transition in our systems compared to environments consisting of saturated ligands (ϵ < 20 M^{-1} cm^{-1}). Because in the normal situation the value of ν_1'' can be very high, the possibility arises that when the minor peak appears on the high-energy side of the maximum, it is still to be assigned to ν_{CT}, though now ϵ for the charge transfer transition is *lower* than it is for what is normally considered a ligand field band. Data taken from Table 6 are displayed in Figure 9. There is such an excellent correlation between the energies of ν_{CT} and ν_1'' when the higher energy transition, whether a shoulder or a maximum, is always assigned to ν_{CT} (Figure 9a) that the conclusion that

(26) Brauer, D. J.; Kruger, C. *Cryst. Struct. Commun.* **1973**, *3*, 421.
(27) Nishio, M.; Hirota, M. *Tetrahedron* **1989**, *45*, 7201 and references cited therein.
(28) Desiraju, G. R. *Acc. Chem. Res.* **1991**, *24*, 290.
(29) (a) Taylor, R.; Kennard, O. *J. Am. Chem. Soc.* **1982**, *104*, 5063. (b) Berkovitch-Yellin, Z.; Leiserowitz, L. *Acta Crystallogr.* **1984**, *B40*, 159.
(30) Martin, L. Y.; Sperati, C. R.; Busch, D. H. *J. Am. Chem. Soc.* **1977**, *99*, 2968.

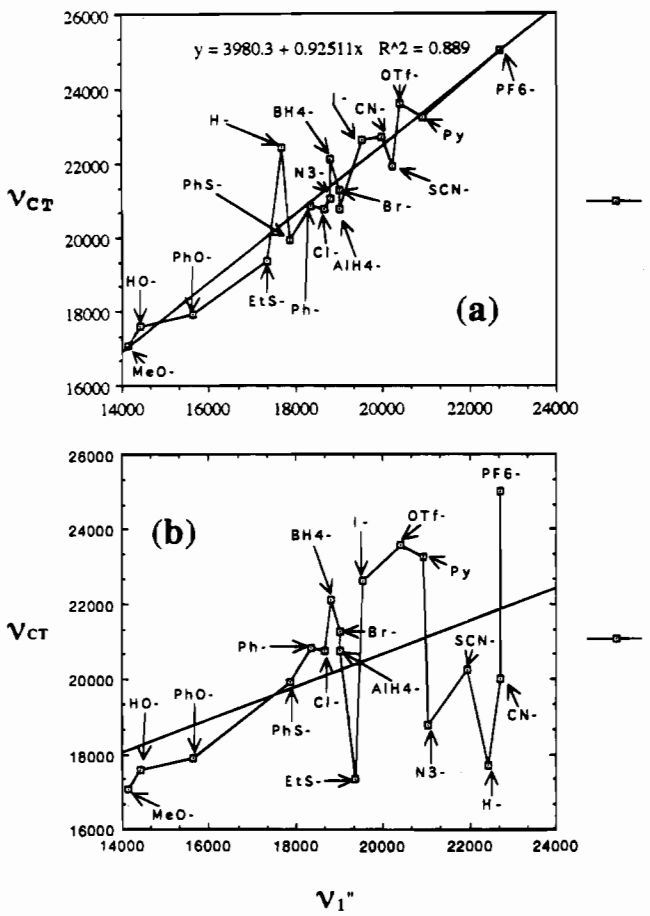

Figure 9. Plot of ν_{CT} and ν_1'' in the $VPy_4(X)_2$ series complexes: (a) high-energy band, whether shoulder or maximum, taken as ν_{CT}; (b) shoulder always assigned to ν_1''. Units for numbers on all axes: cm^{-1}.

ν_{CT} always lies at higher energy than ν_1'' seems inescapable. By contrast, when the maxima are always assigned to ν_{CT}, the correlation is lost (Figure 9b).

The only prominent outlier in Figure 9a is the hydride ion. The ligands CH_3^- and $C_2H_5^-$ are similar to H^- as being among the most nucleophilic bases used in our studies and also in having no capacity for π donation. While we were unable to prepare tetrapyridine complexes of these ligands and as a result, no data for them appear in Figure 9a, the preparation succeeded when 4-ethylpyridine was used as ligand. When the data for $CF_3SO_3^-$, Cl^-, and I^- are plotted as in Figure 9a and a line of unit slope is passed through these points, CH_3^- and $C_2H_5^-$ prove also to be outliers, but appearing below the line and almost as far removed from it as H^- is shown to be in Figure 9a.

The correlation of Figure 9a suggests either that the excited states for ν_{CT} and ν_1'' are rather insensitive to the nature of the axial ligand or that the excited states are shifted equally by a change in the axial ligand (note that the slope of the line in Figure 9a is 0.93). The former seems more likely, considering that in the excited state for ν_{CT} a d electron has been transferred almost completely to a π^* orbital of the ligand, where the effect of the axial ligands on the energy is expected to be small.

The values of ν_{CT} and ν_1'' increase in the order MeO^-, HO^-, PhO^-, EtS^-, PhS^-, $Cl^- \sim N_3^-$, Br^-, I^-, CN^-, SCN^-, $CF_3SO_3^-$, Py and show little relation to the spectrochemical series. To be noted particularly is the reversal in the case of the halide ions. In ordinary circumstances, ν_1'' is taken to measure the ligand field strength of the ligands when the octahedral symmetry is reduced to tetragonal. In the cases of $NiPy_4Cl_2$ and $NiPy_4Br_2$, the values of ν_1'' are 11 730 and 11 490 cm^{-1}, respectively, and thus show the normal order.[31] It is reasonable to suppose that the difference for the two metal ions is associated with the much greater charge transfer from the metal center to π^* orbitals of the ligands for V^{2+} as compared to Ni^{2+}. The ligand order shown suggests that an important influence affecting the energy of the ground state is a net transfer of π-electron density from the axial ligands to the pyridine rings, mediated by the metal ion and made possible by the propeller arrangement of the rings. For a ligand such as HO^-, this will raise the energy of the ground state more than for $CF_3SO_3^-$, where much of the capacity for π donation by oxygen is lost.

As already stated, a striking effect observed in our studies on the pyridine complexes is the enormous enhancement of ϵ for ν_1'' in the V(II)–pyridine species as compared to values observed when only saturated ligands occupy the coordination sphere of V(II). A comparison of $\epsilon(\nu_1'')$ for VPy_4Cl_2 (2.7×10^3 M^{-1} cm^{-1}) with that reported for $NiPy_4Cl_2$ (2.2 M^{-1} cm^{-1})[31] is also relevant. Metal to ligand charge transfer is prominent only in the case of V(II). When, as we infer, ϵ for ν_1'' can in some cases exceed that of ϵ for ν_{CT}, the effect cannot be ascribed simply to "intensity borrowing". For the pyridine complexes of V(II), the transition giving rise to ν_1'' has intrinsic charge transfer character because the extent of metal to ligand charge transfer in the excited state is reduced by the change in orbital symmetry. Also remarkable is the sensitivity of ϵ for ν_1'' to the nature of the ligands, these values covering at least the range from 1×10^2 M^{-1} cm^{-1} for HO^- to 3.5×10^3 M^{-1} cm^{-1} for N_3^- as the axial ligand.

In the early spectrophotometric work[32] on $[Ru(NH_3)_5L]^{2+}$ where L is pyridine or a derivative, the effect of substitution by electron-withdrawing ligands in the 4-position of the pyridine ring was shown to be to lower the energy of the $\pi\delta-\pi^*$ transition. A similar effect is expected for V(II) and is observed. With the ethyl carboxy group as substituent on the 4-position of the pyridine ring, ν_{max} appears at 476 nm, while for pyridine as a ligand, ν_{max} is at 424 nm. It should be noted that, in the case of the substituted pyridine, the low-energy "shoulder", actually a well-defined maximum, has almost the same intensity as the band at higher energy which we assign to ν_{CT}. The comparable values of ϵ for ν_{CT} and ν_1'' lend credence to the conclusion that ϵ for ν_1'' can in some cases exceed that of ν_{CT}.

Substitution by C_2H_5 in the 4-position of pyridine shifts CT to 420 nm, in line with expectation, C_2H_5 being electron releasing compared to H.

The evidence supporting the conclusion that V(II) exists in pyridine as VPy_6^{2+} when PF_6^- and BPh_4^- are counterions seems convincing. In the absence of Jahn–Teller distortions, the six ligands would be expected to occupy equivalent positions around the cation, as is in fact the case for $FePy_6^{2+}$ ($[Fe_4(CO)_{14}]^{2-}$ as anion), where pairs of pyridines lie in planes which are mutually perpendicular.[33] But the general characteristics of the absorption spectrum of VPy_6^{2+} in the region of interest are identical to those observed for the tetrapyridine species, suggesting that axial pyridines in VPy_6^{2+} take the place of the anions, the propeller arrangement of the four equatorial pyridines being retained. Drago et al. reported[34] that the spectral features of a tetragonal distortion are also retained for $NiPy_6^{2+}$ in CH_3NO_2 as solvent when it is generated from $NiPy_4(BF_4)_2$ by the addition of pyridine. The features ν_1' and ν_1'' remain and show small shifts to lower energy in their respective band positions and slight

(31) Rowley, D. A.; Drago, R. S. *Inorg. Chem.* **1967**, *6*, 1092.

(32) Ford, P.; Rudd, D. F. P.; Gaunder, R.; Taube, H. *J. Am. Chem. Soc.* **1968**, *90*, 1187.

(33) Doedens, R. J.; Dahl, L. F. *J. Am. Chem. Soc.* **1966**, *88*, 4847.

(34) Rosenthal, M. R.; Drago, R. S. *Inorg. Chem.* **1965**, *4*, 840.

enhancements in their intensities. Similar red shifts of the transitions are observed in the conversions of $VPy_4(X)_2$ ($X = PF_6^-$, BPh_4^-) to $VPy_6(X)_2$. Unfortunately, we have failed in attempts to grow crystals of the compounds under entries 3 and 5 of Table 6. Experiments, the results of which will be reported separately, on the complexation of V(II) ($CF_3SO_3^-$ as anion) by pyridine in aqueous solution suggest a strongly cooperative effect in the binding of four pyridines, a finding which provides some support to our inference that the pyridines in VPy_6^{2+} are not all equivalent. It is to be noted that ν_{CT} for VPy_6^{2+} appears at much higher energy than that for $V(bipy)_3^{2+}$, 430 nm vs 650 nm,[8d], a difference attributable to the π^* orbitals being at lower energy for bipy than for Py.

The $V(CH_3CN)_6^{2+}$ salts in acetonitrile show only three assignable spin-allowed d−d transitions, consistent with the cation having an octahedral symmetry. The shifts of ν_1 and ν_2 to higher energy are much smaller than observed for isonitriles[8d] or CN^- as ligand. The effects on the spectra of the reduction in symmetry (whether the heteroligands are *cis* or *trans* is not known) arising from the substitution of two acetonitriles by fairly strong nucleophiles, such as Cl^- or Br^-, in the coordination sphere of V(II) ion are found to be very small.[35] It has been observed that the replacement of the two CH_3CN groups in the coordination sphere by Cl^- or Br^- produces a bathocromic shift in both ν_1 and ν_2. While ν_1 for Cl^- or Br^- complexes showed only asymmetric broadening, detectable splitting of ν_2 for the Br^- was observed (see Table 7). As in the case of the tetrapyridine complexes, ν_1'' taken as maximum in the lowest energy envelope for the bromo complex lies at higher energy than that for the chloro complex.

For the $V(DMPE)_2(X)_2$ series, as for $V(CH_3CN)_4(X)_2$, ν_{CT} appears at sufficiently high energy so that the bands arising from ν_1 and ν_2 are clearly resolved from the bands of high intensity associated with charge transfer. The spectral features of the low-energy region (820−380 nm) for the five complexes are shown in Figure 10. The chloro, bromo, iodo, and borohydride complexes display relatively weak absorption ($\epsilon \sim 10-25$ M^{-1} cm^{-1}) in the range 820−710 nm along with a stronger band ($\epsilon \sim 30-70$ M^{-1} cm^{-1}) at ca. 510 nm, the energy of which is almost insensitive to the nature of the axial ligands. It is a reasonable conjecture that the latter band is the result of a superposition of ν_1'' and components of ν_2. This interpretation is supported by observations on the dichloro complex (Figure 10a) where a shoulder, which we assign to a component of ν_2, on the high-energy side of the band in question is clearly discernible. The weaker absorptions at low energies are assigned to ν_1', the energies of which follow the normal sequence $CH_3^- > Cl^- > Br^- > I^-$. It is also supported by the features of the spectrum of $V(DMPE)_2(CF_3SO_3)_2$ where we take ν_1 to lie in the energy region of the first envelope and ν_1'' to correspond to the maximum at 626 nm, the components of ν_2 then accounting for the envelope at the higher energy.

Unusual features in the spectrum of $V(DMPE)_2I_2$ are revealed in Figure 10c. On each side of the prominent band, rather sharp, weak ($\epsilon \sim 1-2$ M^{-1} cm^{-1}) bands appear (702 and 400 nm). These we assign to spin-forbidden transitions which gain intensity from spin−orbit coupling in iodine. Similar effects have been reported for I^- and Br^- as ligands on Cr(III)[36] and Ni(II).[37]

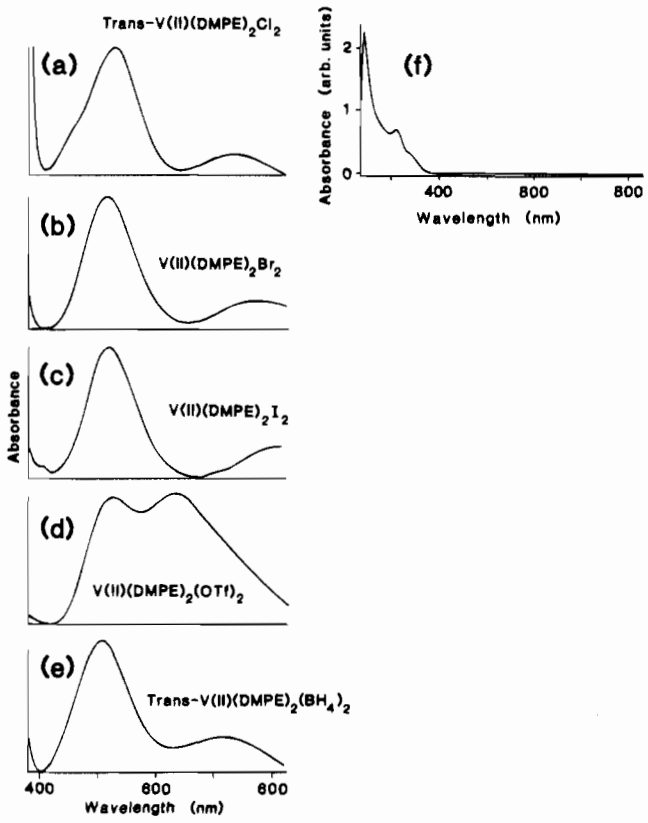

Figure 10. Visible absorption spectra of $V(DMPE)_2(L)_2$ complexes measured in CH_2Cl_2. In (a)−(e) the sensitivity is adjusted to the low-energy region.

Though the intensities of the ν_1'' bands for the acetonitrile and DMPE complexes of V(II) show some enhancements compared those observed for complexes containing only saturated ligands, the effects are very much less than they are for the pyridine complexes. Part of the reason for the difference may be that pyridine is a stronger π acid than either CH_3CN or DMPE. As a result, there is less metal to ligand charge transfer in the ground state for the latter and a smaller change in dipole moment on excitation.

Electrochemistry. Where values of $E_{1/2}$ were obtained, the change in $E_{1/2}$ with the nature of the axial ligand provides information on the relative affinities of a particular ligand for VPy_4^{3+} as compared to VPy_4^{2+}.

Because the reversible potential ($E_{1/2}$) for the solvento species is not known (only E_{pa} is registered), we will use $V(Py)_4CF_3SO_3)_2^{3+/2+}$ as the reference couple, chosen because the value of $E_{1/2}$ for it is at an extreme—in this case, as the most highly oxidizing. The affinities of the ligands for V(III) as compared to V(II) increase in the order $CF_3SO_3^-$ (0), I^- (0.40), SCN^- (0.44), Br^- (0.48), AlH_4^- (0.59), BH_4^- (0.72), Cl^- (0.73), Ph^- (0.70), N_3^- (0.91), H^- (1.05). The numbers in parentheses are the values of $\Delta E_{1/2} = E_{1/2}$(reference couple) − $E_{1/2}$(variable ligand couple). The entry for I^-, for example, represents nE° (we take $E_{1/2}$ to be equivalent to E°) for the reaction

$$VPy_4(CF_3SO_3)_2^+ + VPy_4I_2 = VPy_4(CF_3SO_3)_2 + VPy_4I_2^+ \quad (1)$$

and shows that I^- as compared to $CF_3SO_3^-$ strongly favors association with V(III) over V(II). When $\Delta E_{1/2}$ is converted to the equilibrium constant for the reaction above by the relation $\log K(25\ ^\circ C) = \Delta E_{1/2}/0.0593$, the value of K in the case of I^- is 6.3×10^6. Among the ligands we have studied, H^- most strongly stabilizes V(III) over V(II), and K for the corresponding

(35) (a) Lever, A. P. B. *Coord. Chem. Rev.* **1968**, *3*, 119. (b) Wentworth, R. A. D.; Piper, T. S. *Inorg. Chem.* **1965**, *4*, 709. (c) Krishnamurty, R.; Sehapp, B. W.; Perumareddi, J. R. *Inorg. Chem.* **1967**, *6*, 1338. (d) Perumareddi, J. R. *J. Phys. Chem.* **1967**, *71*, 3155.

(36) (a) Pedersen, E.; Toftlund, H. *Inorg. Chem.* **1974**, *13*, 1603. (b) Linhard, M.; Weigel, M. *Z. Anorg. Allg. Chem.* **1951**, *266*, 49.

(37) Nelson, S. M.; Shepherd, T. M. *Inorg. Chem.* **1965**, *4*, 813.

reaction in this case is 2.8×10^{17}. The order for the halides is that expected for oxophilic centers, Cl^- showing a much greater preference for V(III) over V(II) than does I^-. A surprising result is the very high discrimination by N_3^- in stabilizing V(III) over V(II), much greater than that of SCN^-. Hydride has already been noted as being the most effective of all the anions in stabilizing the higher oxidation state over the lower. As expected, the capacity of H^- in this respect is much reduced when it is coordinated to the Lewis acid BH_3 or AlH_3 but the relative order indicates that AlH_3 in association with H^- is more strongly electron-withdrawing than BH_3, a result which we find surprising. It should be noted that the value of $E_{1/2}$ for V(4-EtPy)$_4$(BH$_4$)$_2$ is quite close to that recorded for VPy$_4$(BH$_4$)$_2$, suggesting that both are on a sound basis.

When we deal with values of E_{pa}, we are on weaker grounds in making comparisons of relative affinities, but it seems unlikely that the bias introduced by the use of E_{pc} rather than $E_{1/2}$ will exceed 0.20 V. Thus the decrease in E_{pa} when PF_6^- or BPh_4^- is replaced by pyridine—1.03 V to 0.63 V—almost surely reflects a greater capacity of pyridine to stabilize V(III) over V(II) as compared to the very weak nucleophilic anions. It is unlikely that pyridine in the axial positions engages in much back-bonding stabilization of V(II), and it is a rather good σ donor, thus favoring association to V(III) over V(II).

The close correspondence of the spectra of VPy$_4$(O$_3$SCF$_3$)$_2$, **1**, in pyridine and in CH_2Cl_2 makes it almost certain that in each solvent the anions are ligated to V(II). It is to be noted that, even for the weaker nucleophile BPh_4^-, dissolution of a tetrapyridine solid in CH_2Cl_2 does not lead to displacement of the anion (see entry 4, Table 6). The only possibility then to explain the extra prominent cyclovoltammetric signal at E_{pc} = 0.97 V when [^{t}Bu$_4$N]PF$_6$ (0.10 M) is added to a solution of **1** in pyridine appears to be that VPy$_4$(O$_3$SCF$_3$) (PF$_6$) is formed. This is consistent with the observation that when [^{t}Bu$_4$N]O$_3$SCF$_3$ is the electrolyte, though a wave at 0.97 V is still observed, it is much weaker in intensity than when the PF_6^- salt is used. However, what is difficult to understand is that, even in the presence of the [^{t}Bu$_4$N]O$_3$SCF$_3$, an extra (though small) electrochemical signal is observed, which would on the face of it, contradict the conclusion that, in the absence of electrolyte, VPy$_4$(O$_3$SCF$_3$)$_2$ is by far the dominant form in solution. The resolution for the difficulty may be in recognizing that if the electrolytes are largely ion-paired (or clustered), the common ion effect as we know it in solvents of high dielectric constant does not obtain. In fact, the argument could be made that an ion pair such as [^{t}Bu$_4$N]$^+$·[O$_3$SCF$_3$]$^-$ would favor [VPy$_5$(O$_3$SCF$_3$)]$^+$·[O$_3$SCF$_3$]$^-$ over VPy$_4$(O$_3$SCF$_3$)$_2$ because of the higher dipole moment of the former structure. It needs to be recognized that if ion pairing prevails, adherence to Beer's law for a solution of VPy$_4$(O$_3$SCF$_3$)$_2$ in pyridine contributes nothing to distinguishing between VPy$_4$(O$_3$SCF$_3$)$_2$ and [VPy$_5$(O$_3$SCF$_3$)]$^+$. When the latter is formulated as the ion pair [VPy$_5$O$_3$SCF$_3$]$^+$·[O$_3$SCF$_3$]$^-$, it is evident that the two species differ only in content of pyridine and the activity of the solvent is almost unchanged by dilution.

It is worth emphasizing that, in contrast to the reactions of $V(H_2O)_6^{2+}$ in H_2O, where the half-time at room temperature for substitution with ligands at the concentration level used in these studies is of the order of seconds, in pyridine the half-times can be minutes or even hours. It is obvious that the kinetics of substitution in many cases could be studied without resort to sophisticated techniques.

Finally, we draw attention to the values of $E_{1/2}$ for V(4-EtPy)$_4$(O$_3$SCF$_3$)$_2$, VPy$_4$(O$_3$SCF$_3$)$_2$, and V(ethyl isonicotinate)$_4$(O$_3$SCF$_3$)$_2$, 0.50, 0.67, and 0.94 V, which do seem to reflect back-bonding stabilization by the equatorial pyridines of V(II) relative to V(III).

Even though, in CH_3CN as solvent, in no case were we able to obtain values of $E_{1/2}$, the values of E_{pa} being so much higher than for the corresponding couples in pyridine, it seems safe to conclude that CH_3CN stabilizes V(III) relative to V(II) less than does pyridine. This applies in the kinetic as well as the thermodynamic sense and is in the line with the lower nucleophilic power of CH_3CN. DMPE, on the other hand, stabilizes V(III) relative to V(II) more than does pyridine. Contributions by back-bonding in the case of the phosphine are likely quite small. In any event, they would stabilize the lower oxidation state more than the higher; apparently the nucleophilic power of the phosphorus atom is great enough to overcome any such effects.

Acknowledgment. The authors express their appreciation for financial support of this research by the NSF (Grant No. CHE 9120158-A01). We are grateful to Professor Edward Solomon for giving us the opportunity to run the computer programs for Gaussian resolution of the spectral data.

Supporting Information Available: Text giving further details of the structure determination, tables of atomic coordinates for the hydrogen atoms, intramolecular distances involving the non-hydrogen atoms, intermolecular distances involving the non-hydrogen atoms, intramolecular bond angles involving the non-hydrogen atoms, torsion or conformation angles, and least-squares planes, and a listing of microanalytical results for all complexes reported in the text (22 pages). Ordering information is given on any current masthead page.

IC9503848